SKB

TECHNICAL REPORT 88-15

Hydrothermal effects on montmorillonite

A preliminary study

Roland Pusch, Ola Karnland

Clay Technology AB, Lund, Sweden

June 1988

SVENSK KÄRNBRÄNSLEHANTERING AB
SWEDISH NUCLEAR FUEL AND WASTE MANAGEMENT CO

BOX 5864 S-102 48 STOCKHOLM
TEL 08-665 28 00 TELEX 13108-SKB

HYDROTHERMAL EFFECTS ON MONTMORILLONITE

A preliminary study

Roland Pusch, Ola Karnland

Clay Technology AB, Lund, Sweden

Juni 1988

CLAY TECHNOLOGY AB

ID-no: CTRAP 8801
Date: 1988-06-01

HYDROTHERMAL EFFECTS ON MONTMORILLONITE

-

A preliminary study

Roland Pusch
Ola Karnland

Clay Technology AB
Lund, Sweden

Keywords: Bentonite, brammalite, clay, microstructure, montmorillonite, hydrothermal treatment, hydrous mica, illitization, paragonite, smectite

CONTENTS

SUMMARY

Hydrothermal effects on montmorillonite clay are usually taken to have the form of conversion of this clay mineral to other species, such as illite, disregarding microstructural alteration and cementation caused by precipitation of silica and other compounds. The present report is focussed on identification of the primary processes that are involved in such alteration, the release of silica and the microstructural changes associated with heating being of major interest. In the first test phase, reported here, Na montmorillonite in distilled water was investigated by XRD, rheology tests and electron microscopy after heating to 60-225°C for 0.01 to 1 year.

The preliminary conclusions are that heating produces contraction of the particle network to form dense "branches", the effect being most obvious at the highest temperature but of significance even at 60-100°C. Release of substantial amounts of silica has been documented for temperatures exceeding 150°C and precipitation of silica was observed on cooling after the hydrothermal testing under the closed conditions that prevailed throughout the tests. The precipitates, which appeared to be amorphous and probably consisted of hydrous silica gels, were concluded to have increased the mechanical strength and caused some brittleness, particularly of the dense clays.

The nature of the silica release, which is assumed to be associated with beidellitization, may be closely related to an unstable state of a certain fraction of tetrahedral silica at heat-induced transfer between two different crystal modes of montmorillonite.

1 SCOPE OF STUDY

Smectite clay like MX80 Na bentonite, used as canister envelope or as plugs or rock grout, will be exposed to a temperature cycle and rather high water pressure following a scenario which also involves exposure to water vapor. This may influence the stability of the clay in two ways which affect the sealing ability: 1) the crystal lattices may undergo permanent changes resulting in a largely reduced swelling and gel-forming capacity, and 2) the microstructure may become temporarily or permanently altered by which the hydraulic conductivity and diffusivity can be significantly changed. These effects are presently being investigated in a study that covers the complete thermomechanical scenario in a repository.

The present report gives preliminary data from exploratory hydrothermal tests for identifying major alteration processes and for developing suitable cells for heat treatment of "closed" smectite/water systems. Both low-density and high-density Na montmorillonite clays are included in the study, which covers the temperature range 20 and 225°C and water pressures ranging from less than 1 MPa to about 70 MPa.

2 INTRODUCTION

Safe prediction of the isolation power of smectite-based clay materials in HLW repositories requires that their major physical properties are preserved or that possible changes can be quantitatively determined and modelled. These properties, i.e. the hydraulic conductivity, ion diffusivity and expandability, can be changed by non-reversible chemical alteration of the clay mineral crystals and microstructural reorganization. The first-mentioned type of alteration, particularly concerning heat effects, has been and is still being investigated in various international projects, while the matter of quantitative microstructural changes associated with heating and variations in porewater chemistry, has hardly been considered yet. Both types of alteration will be touched upon in this report.

3 HYDROTHERMALLY INDUCED CHANGES OF SMECTITE MINERALS

3.1 GENERAL

The crystal structure of smectite consists of two layers of tetrahedra - principally Si with minor Al - sandwiched to the top and bottom of a layer of octahedrally coordinated cations, usually Al but with some Mg and Fe. The structure is apt to undergo alteration on environmental changes in the form of heat-induced replacement of a significant fraction of the tetrahedral silica by aluminum, and possibly by loss of octahedral aluminum. This yields a very significant charge change, which is a first step in possible mineral transformations and altered hydration properties of the material. The release of silica may be closely related to a transfer from a "low temperature" form of montmorillonite, in sodium or lithium state, to a "high temperature" version. This matter is a key question that needs much attention.

In this first chapter an attempt is made to sort out current major views and to present preliminary results from a first hydrothermal laboratory test series. Since a number of tests are in progress, the statements and conclusions are preliminary. However, as described in this paper, it is the authors' feeling that some of the basic heat-related mechanisms in montmorillonite clay are now at least partly understood.

3.2 CURRENT VIEWS

3.2.1 Solid/solid transition

For the particular case of pH ranging from about 7 to 10, a great number of investigators have suggested a solid solution-type, heat-induced conversion mechanism in which illite forms from smectite through tetrahedral substitution and interlamellar uptake of potassium (1, 2, 3, 4). A general expression of the reaction has the form in Eq. (1):

$$Montmorillonite + Al^{3+} + K^{+} \rightarrow Illite + Si^{4+} \qquad (1)$$

This conversion scheme implies that a charge change is produced through replacement of tetrahedral silica by aluminum originating either from octahedral lattice positions or from external sources, and that no actual dissolution takes place, except that silica is liberated. The mineral so formed is beidellite, the charge change being balanced by adsorbed cations. If potassium ions are available they become fixed in conjunction with interlamellar collapse yielding illite.

In terms of Maegdefrau's general formula, the mineral created by the replacement of tetrahedral silica by aluminum and interlamellar uptake of monovalent cations to balance the charge change, would be:

$$M^{I}_{y}\, Si_{(8-y)}\, Al_{y}\, O_{20}\, (OH)_4\, (M^{III}, M^{II})_4 \qquad (2)$$

where y is in the range of 1-2, M^{I} represents monovalent cations, M^{II} magnesium and divalent iron and M^{III} aluminum or trivalent iron. Electrostatic forces, hydrogen bonds and mass forces keep the layers together. If K^+ is available in sufficient concentration, illite will ultimately be formed, while absence of potassium means that the smectite is preserved in beidellite form. It exhibits similar expansion properties as montmorillonite on hydration/dehydration, and does not collapse permanently with other cations than K^+ in the interlamellar space. It is possible that certain conditions, like high pressure and temperature, may yield collapse of sodium-saturated beidellite to non-expanding 10 Å-minerals of paragonite-type such as brammalite ("sodium-illite").

By applying thermodynamics to montmorillonite in polyelectrolyte solutions, Tardy and Touret (5) recently demonstrated that different cations are taken up in interlamellar positions at different degrees of water saturation. Assuming that "dry" conditions are equivalent with heavy compaction, they concluded that potassium is preferred to sodium in very dense smectite clay while the opposite is valid for "soft" conditions.

3.2.2 Dissolution/neoformation

In 1985 Pollastro suggested a model according to which illite is formed by partial dissolution of smectite components of expandable I/S aggregates and precipitation of dissolved species on low-expandable aggregates (6). The same year Nadeau et al (7) suggested a somewhat similar alteration mechanism for the conversion of

smectite to illite and their idea is supported, in a general sense, by other studies, such as the comprehensive investigation of the Shinzan area in Japan by Inoue et al (8) and by Güven's (9) electron microscopy investigations which indicated that heat-exposed smectite has two major forms: a flakey or mossy appearance representing interstratified I/S, and lath-shaped minerals representing illite that has grown in the pores (Fig 1). The latter objects are supposed to be formed by precipitation of components dissolved from the smectite, in which the potassium content is successively altered. In principle, the creation of both I/S alteration products and neoformed "illite" can be explained by Boles and Franks' illitization reaction in Eq. (3), which implies that some of the smectite is consumed through "cannibalization".

$$\begin{aligned} &3.93\,K + 1.57\,KNaCa_2Mg_4Fe_4Al_{14}Si_{38}O_{100}(OH)_{20}, 10\,H_2O \rightarrow \\ &5.5Mg_2Fe_{1.5}Al_{22}Si_{35}O_{100}(OH)_{20} + 1.57\,Na^+ + 3.14\,Ca^{2+} + \\ &4.28\,Mg^{2+} + 4.78\,Fe^{3+} + 3.14\,Ca^{2+} + 4.28\,Mg^{2+} + \\ &4.78\,Fe^{3+} + 24.66\,Si^{4+} + 57\,O^{2-} + 11.40\,OH^- + 15.7\,H_2O \end{aligned} \qquad (3)$$

This reaction requires that potassium is available for transformation of montmorillonite to illite and it implies that the first-mentioned mineral is extremely stable provided that the potassium content remains very low (cf. 10). The fact that beidellite forms from montmorillonite on heating demonstrates, however, that one of the major reaction steps in the transformation of this mineral to illite takes place also in the absence of potassium and therefore that the dissolution/reformation process and K-uptake may follow quite different paths.

The present authors consider it to be possible that complete lack of potassium and a high concentration of sodium in the porewater may also yield collapsed 10 Å-type minerals on strong dehydration caused by pressure or high temperature. Theoretically at least, this could promote formation of brammalite ("sodium illite") or mixed layer minerals consisting of brammalite/smectite. These analogous processes have not been proposed in the literature although there are examples of mixed-layer brammalite/smectites (11, 12). At very low salinities intravoid neoformation of phyllosilicates in smectites does not take place on heating.

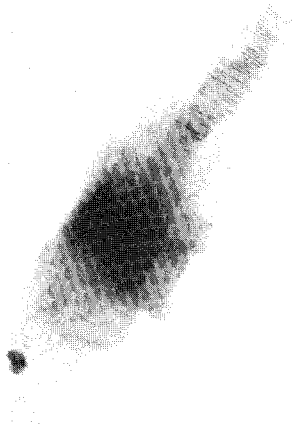

Fig 1 Transition of illite laths into platelets in hydrothermally treated smectite clay. Magnification 20 000X (Photo: N. Güven)

3.2.3 Reaction rates

It is usually assumed that the crystal lattice reorganization of smectites yielding illitization is a true Arrhenius-type kinetic process (13). This philosophy was also applied by Pytte, who made a comprehensive field study and related it to conventional rate expressions in order to evaluate the activation energy of the illitization. His empirical syntheses based on geological data from illite/smectite suites of Cretaceous and Tertiary age (Pierre shale, Colorado, and Dulce siltstone, New Mexico, respectively) led to the conclusion that kinetic factors control the dissolution reaction progress (10). XRD plots of I/S clay samples taken at different distances from the interface between clay-bearing strata and diabase intrusives were compared with I/S-distributions derived by use of the rate law in Eq. (4):

$$-dS/dt = (Ae^{-U/RT(t)})(\{K+\}/\{Na+\})^{m}S^{n} \qquad (4)$$

where S equals the mole fraction of smectite in I/S assemblages, R is the gas constant, T the absolute temperature, t is time, and m and n indicating different order equations. Using back-calculated temperature histories good agreement was obtained with the XRD data by setting *m* equal to unity and *n* equal to 3,4 or 5. The activation energy was found to be in the range of 27 to 33 Kcal/mole, which is higher than the values derived by Eberl and Hower (14) on the basis of hydrothermal tests (19.6 Kcal/mole) but on the same order of magnitude as the activation energy obtained by Roberson and Lahanne (15). Fig.2, which illustrates the illitization rate for the activation energy 27 Kcal/mole, leads to the conclusion that a temperature of 60°C would not yield a noticeable illite content in 100 000 years in a closed system with K-bearing minerals, while 130°C would convert most of the smectite to illite in about 1000 years. At 150°C significant illitization would be expected in 10 to 50 years and at 225°C one would find 30-50 percent of the smectite to be illite in a few months. Such transformation rates would be compatible, in principle, with the reaction model implying dissolution of the smectite and neoformation of illite, while it is not clear whether the charge change solid reaction that produces beidellitization exhibits the same kinetic pattern or if it is an Arrhenius-type reaction at all. It may well be that the I/S distributions observed by Pytte may result from different contents of beidellite at different distances from the hot diabase intrusions, the exchange of tetrahedral silica by octahedral aluminum that produces this mineral form being a very rapid process. Such a scenario would actually be supported by the results obtained by Howard and Roy (16), who derived the activation energy value 3.5 Kcal/mole for K-saturated collapse of hydrothermally treated montmorillonite. The clay exposed to heat had been saturated with solutions with Na as dominant cation (total cation content 197 - 260 ppm), the water content being 2500 %, the water pressure 30 MPa and the temperature 150 and 250°C in different experiments. The very low activation energy arrived at does not indicate crystalline reorganization involving disruption of Si-O and Al-O bonds but merely breakage of hydrogen bonds, which may actually be involved in the conversion of montmorillonite to beidellite as shown later in this report. In this context it is worth mentioning that their experiments at 250°C produced only half as much silica as available, while 150°C gave congruent dissolution of the montmorillonite, indicating that beidellite had been formed in the temperature range 150-250°C.

As concerns the simple solid-solid transformation one concludes that once the charge change leading to beidellitization has taken place, the transformation to illite may simply be a matter of time, and the actual rate of alteration being deter-

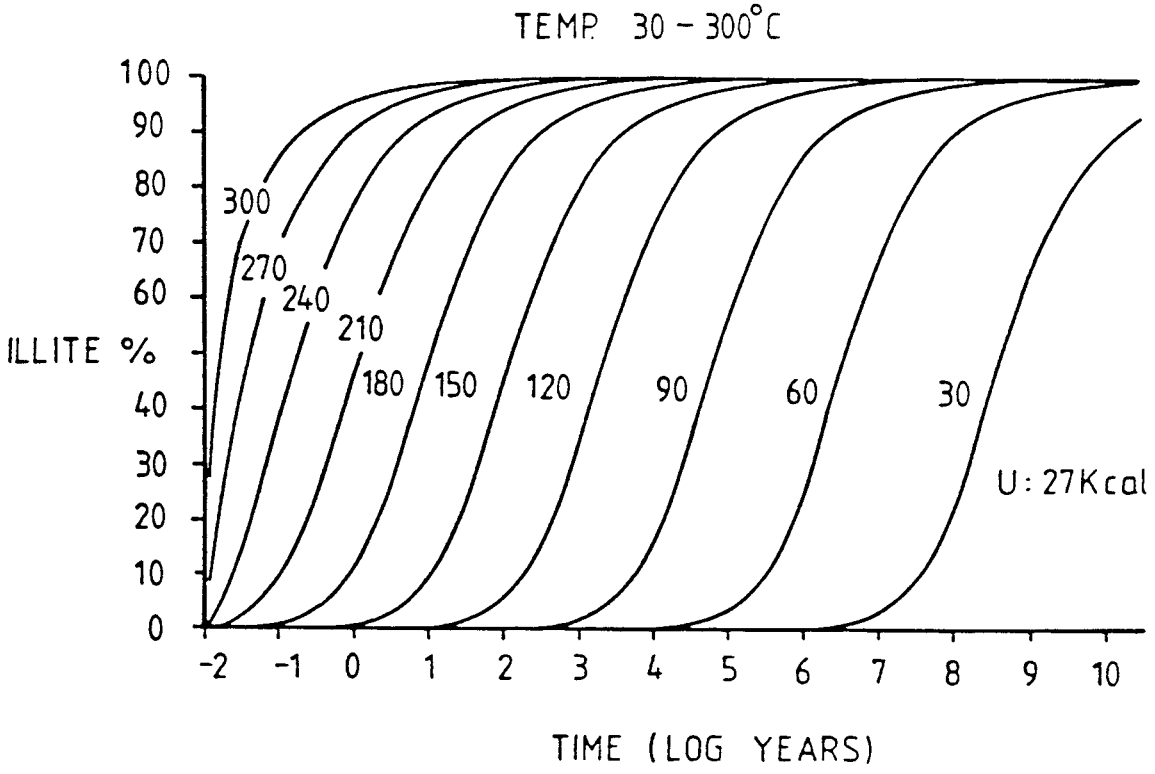

Fig 2. Illitization rates at different temperatures (9)

mined by the rate of dissolution of K-bearing minerals in the clay, or by the rate of transport of dissolved potassium to the clay through percolating groundwater or through diffusion. It is realized that both can be very much retarded in nearfield canister embedment as illustrated by examples given by Duwayne M. Anderson (17). Thus, applying a cation exchange capacity of 70 meq/100 g clay, a potassium concentration of 20 ppm, a hydraulic conductivity of the clay of 10^{-11} m/s, and a thickness of percolated, dense Na smectite of 0.1 m, complete conversion to illite would take about 1 million years provided that the hydraulic gradient is 0.1. Although calculations of this sort are not altogether conservative because of the fact that potassium-bearing water will flow 10 to 100 times faster through a small number of continuous passages (17) from which lateral diffusion takes place, it indicates that the smectite content - in beidellite form - would remain high for very long periods of time.

3.3 DISCUSSION

As to mineral transformation at medium pH, one concludes that the reactions leading to partial or complete transformation of smectite to hydrous mica will affect the character of the particle network, particularly the microstructure and the rheological properties. From a practical point of view the two major types of reactions, i.e. the simple solid/solid transition with internal crystal reorganization and potassium uptake, and the dissolution/neoformation, are expected to yield different physical properties with respect to hydraulic conductivity and swelling ability. Thus, if the total volume is kept constant, the first-mentioned alteration would lead to collapse of the interlamellar space and to a very significant increase in pore size and content of "external water" (cf.18) by which the hydraulic conductivity would be significantly increased, and the swelling pressure strongly reduced. The second type of reaction with neoformation of illite in the pores may partly reduce the effect of smectite dissolution so that the hydraulic conductivity is only slightly enhanced and the swelling pressure moderately reduced.

It is not clear, however, what effect the released silica will have or what the detailed mechanisms are in the release process. It has been assumed by the senior author that the release of silica takes place in conjunction with heat-induced collapse of apical tetrahedrons of the "low temperature" montmorillonite (Edelman/Favejee) crystal structure (18) and that the dissolved silica may be precipitated in the form of an amorphous hydrated silica gel at the edges of montmorillonite stacks (Fig 3). The Ordovician Kinnekulle bentonite was suggested as a possible example since electron microscopy has shown that this clay has a high frequency of precipitation "nodules" (Fig 4), which were taken to be silica compounds resulting from heat-induced release and precipitation of silica originating from the montmorillonite lattices, since earlier investigations using optical microscopy have indicated the presence of minute quartz rims on bentonite grains (19).

Conodont analyses and back-calculation of the heat flow from a basalt intrusion have shown that the temperature averaged at 110°C at minimum and 160°C at maximum for 1000-2000 years, which would indicate that release and precipitation of silica takes place at temperatures around 150°C. The central portion of this I/S- rich 2 m thick Kinnekulle clay bed is less illiticized than its upper part as documented by a higher potassium content and a lower swelling ability of the

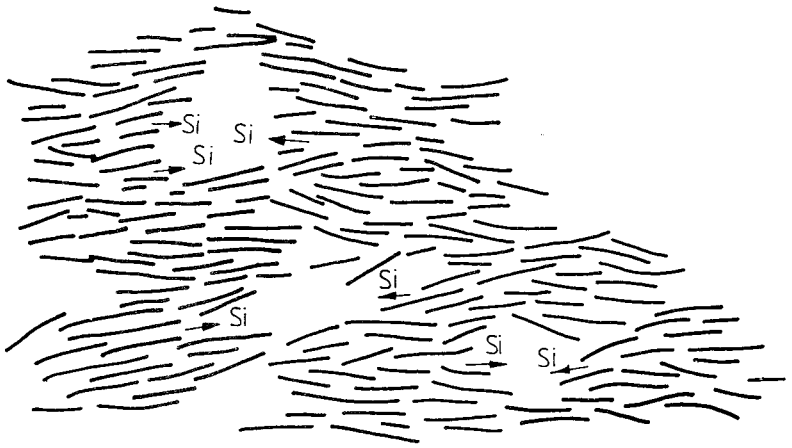

Fig 3. Schematic smectite flake arrangement in natural bentonites. Arrows indicate assumed Si migration at heating

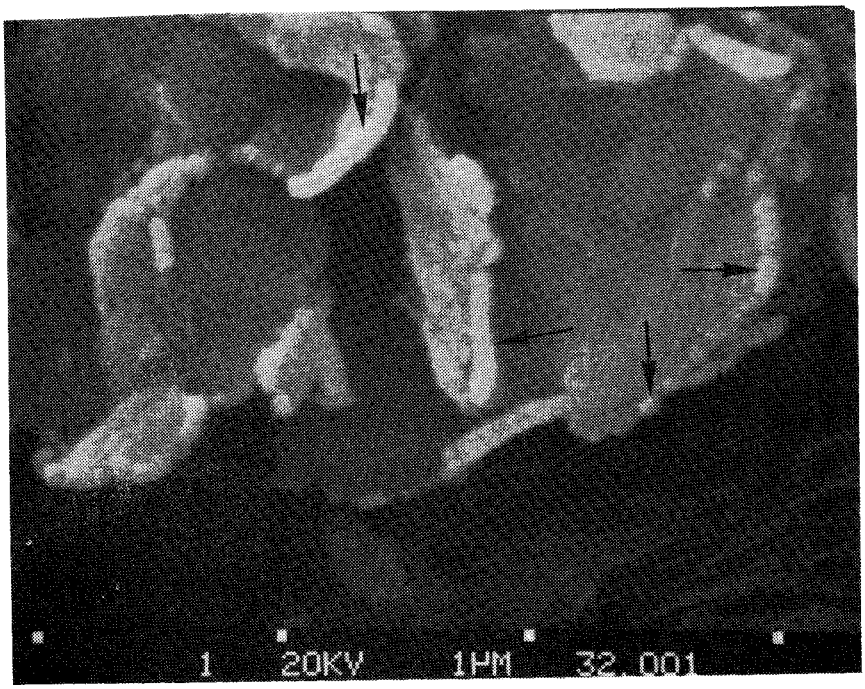

Fig 4. Presumed silica precipitations in Kinnekulle clay as observed by use of SEM (gold-sputtered, freeze-dried specimens). The size of the nodules is generally in the range of 0.03-0.08 μm

latter (18, 19, 20). Since the entire bed must have been exposed to practically the same temperature, the different degree of illitization is related either to slower (heat-aided) diffusion to the central part from external K-rich sources or to different initial contents of K-bearing minerals.

The precipitation of silica, which must be strongly dependent of the concentration of dissolved silica in the porewater of the bentonite clay as discussed later in the report, may be very significant. Thus, about 25 % of all silica will be released solely on transformation of montmorillonite to beidellite and since this corresponds to at least 10 % of all solid matter it should affect the rheological properties substantially if the precipitates serve as cement. Actually, precipitation of only 1-3 % solid substance in cementitious form is known to have a strong effect on the mechanical properties of most soils and we find this to be true also for the Kinnekulle clay as demonstrated by the graphs in Fig 5. Thus the curve for the second load step in log γ /log t plotting exhibits the slight upward concave shape (negative t_0) that is characteristic for loads that are sufficiently high to initiate breakdown of cementation bonds. One finds that the lowest shear stress 55.5 kPa, which left the majority of the cementing bonds intact, gave very small strain and the usual log time creep with positive t_0. The highest load yielded creep of almost constant rate, which suggests that creep failure was approached.

Further information on silica precipitation has been offered by a large scale field heating experiment, in the Stripa mine, i.e. the the so-called BMT test (21). It was conducted a few years ago, the purpose being to investigate whether the chemistry and physical properties of dense, almost completely water saturated Na bentonite would be altered in one year at 125°C under low water pressure conditions (300-700 kPa). The water had sodium as major cation and the ion strength was very low. The analyses comprised XRD and chemical analyses as well as electron microscopy and determination of two characteristic physical properties, i.e. the swelling pressure and the hydraulic conductivity. It was found from this comprehensive study that the only alterations that could be identified were a very slightly reduced swelling capability as observed by use of XRD technique and traces of precipitations at the edges of certain montmorillonite aggregates (Fig 6). Probably these effects were caused by vapor attack in the non-saturated bentonite close to the clay-embedded heaters, which were located in large-diameter boreholes.

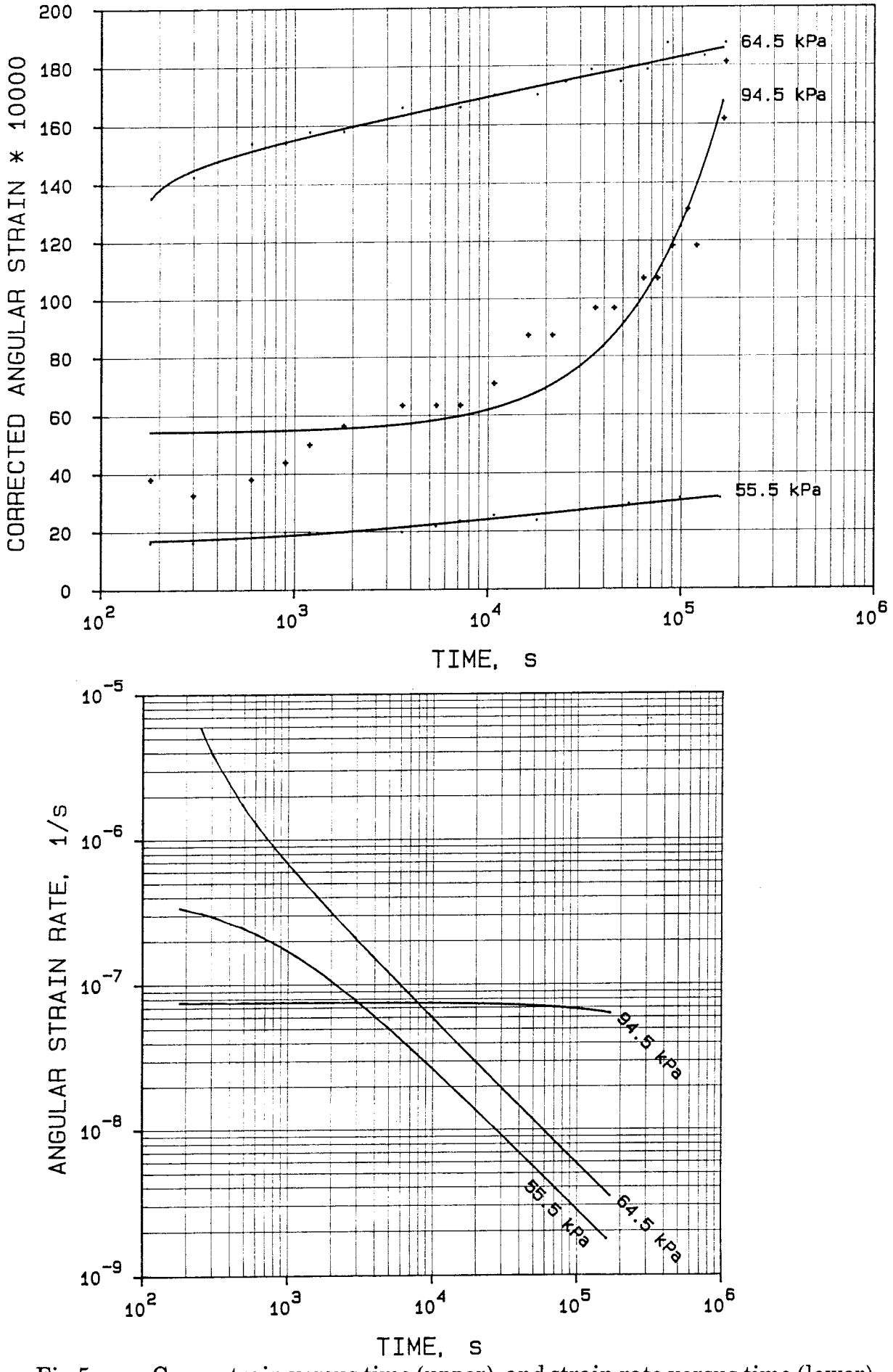

Fig 5. Creep strain versus time (upper), and strain rate versus time (lower) of Kinnekulle bentonite

Slight beidellitization could possibly have taken place but neoformation of hydrous mica minerals had definitely not occurred. The fact that boehmite was identified close to the heaters points to dissolution of iron from iron-holding minerals, like pyrite.

The conclusion of all these considerations is that release of silica is a primary mechanism in heat-induced alteration of montmorillonite as specified by Eq.(1) and that hydrothermal tests, conducted at temperatures ranging between 60 and about 200°C and with a duration of 0.1-1 years, would give detailed information on:

1) Heat-generated formation of silica precipitates per se

2 The art of energy dependence of silica release: Arrheniusian or critical temperature dependent release of silica

The first part of our experimental study therefore comprised a series of hydrothermal tests with the aim of identifying the silica cycle in montmorillonite clay exposed to heat and pressure under physically and chemically closed conditions.

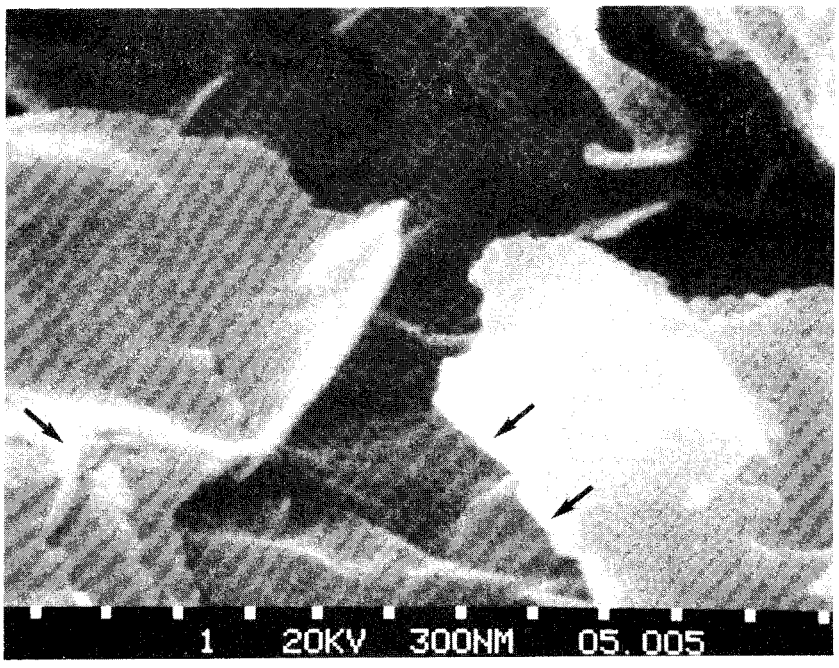

Fig 6. SEM micrograph of MX 80 Na bentonite from the BMT test. Collapsed stacks of flakes with a few precipitation nodules at the edges of the stacks. The nodules have a size in the range of 0.005-0.05 μm

4 HYDROTHERMALLY GENERATED MICROSTRUCTURAL CHANGES OF SMECTITE CLAYS

4.1 BASIC CONCEPTS

As for most other clay types, the multiple-plate microstructure concept holds also for Na montmorillonite (22). Thus, this type of smectite clay consists of stacks which are thick and comprise several flakes at high bulk densities and which persist after expansion but with a smaller number of flakes (Fig 7). It is concluded from ongoing studies that the continuity of the particle network is preserved even at large expansion, which has a great impact on the erodablity of soft gels such as those used for rock grouting.

The interaction between montmorillonite flakes and interlamellar water is concluded to give this ordered, "internal" water an energy state that is similar to that of ice (18). Probably, only 2 or 3 hydrates are hosted in each interlamellar space and they remain immobile between the flakes even at high hydraulic gradients. Thus, only "external" water in continuous voids is expected to flow under the influence of differential piezometric heads. The location of this mobile water is determined by the microstructure.

For the sake of simplicity we will still use the term particle for individual microstructural constituents in the subsequent text together with the specifications "flake" and "lamella" for individual crystal sheets, "stacks" for aligned, regularly ordered sheets, and "aggregate" for coherent groups of non-oriented sheets and stacks.

Since many of the practical repository sealing operations imply that Na bentonite powder is used in the form of compacted blocks, it is pertinent to consider the microstructure of such "artificially" produced clays. The individual grains consist of large numbers of more or less aligned stacks of montmorillonite flakes but since the grains are randomly oriented in the powder mass the orientation of flakes is approximately at random also in the saturated state. The homogenization, or maturation process, which is schematically illustrated in Fig 8, results in a microstructural arrangement of the type shown in Fig 9 when the dry density is in the range of 0.9 to 1.8 t/m^3. The dense "I"-bodies have an internal structure like the upper arrangement in Fig 7, while the softest gels in external pores are structurally organized like the lower arrangement in this figure. This model implies that

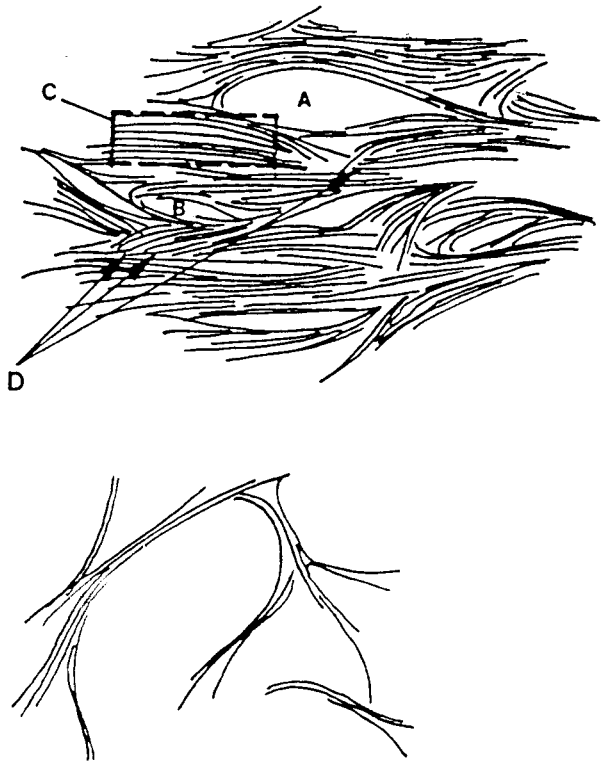

Fig 7. Upper: Dense Na montmorillonite clay. A) Large pore, B) Small void with external water, C) Stack or "quasicrystal" with organized interlamellar water, D) Interface between stacks. Lower: Expanded Na montmorillonite gel with very thin stacks and practically only external water

there are variations in homogeneity which account for significant changes in hydraulic conductivity and diffusivity on alteration of the porewater chemistry and the temperature.

4.2 INTERNAL/EXTERNAL PORE SPACE

It is of fundamental importance to distinguish between interlamellar space holding "internal" water, and voids which host "external" water (18). The first-mentioned space contains immobile, interlamellar water that forms a large fraction of the total pore volume in smectite-rich clays of high density, while it

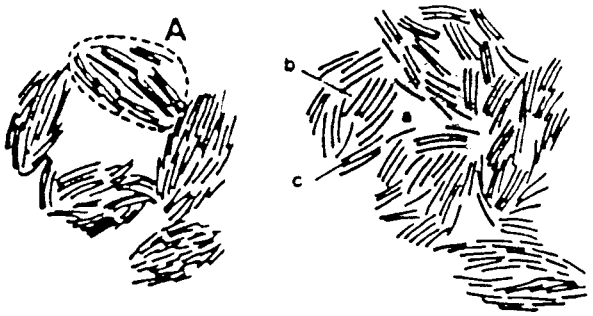

Fig 8. Schematic particle arrangement in highly compacthed Na bentonite. Left picture: powder grains in air-dry state. Right picture: "homogeneous" state after saturation and particle redistribution. A = grain consisting of stacks of flakes, a and b = voids of various size, c = interlamellar space in stack

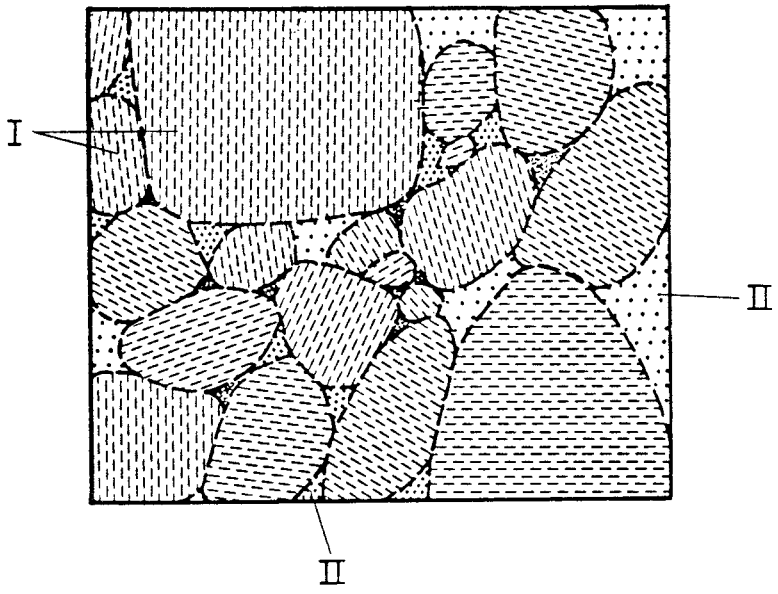

Fig 9. Generalized microstructural pattern of Na montmorillonite clay gel formed from powder grains. I is expanded grain (1-3 interlamellar hydrates), II external pores with gels of different densities

only represents a minor part at average dry densities lower than about 0.5-0.6 t/m^3 (Fig 10). Naturally, a much larger number of voids combine to form passage-ways for water or gas in soft than in very dense smectite clays. It has been

estimated that for an average dry density of 0.8-1.1 t/m^3, about 5-10 % of an arbitrary cross section hold relatively soft clay gels ($\rho_d = 0.15$-0.5 t/m^3) with a significant content of mobile water and that only about 0.5-2 % hold very open gels ($\rho_d < 0.15$ t/m^3). It is reasonable to believe that the last-mentioned microstructural components form pore fillings that are very permeable, but since the degree of interconnectivity is higher of the clay gel of "intermediate permeability", i.e. the one with a dry density of 0.15-0.5 t/m^3, the latter is probably a determinant of the percolation of water. For compact clays having a dry density exceeding 1.1-1.3 t/m^3 the clay gel of intermediate permeability is assumed to form only 0.5-1 % of the total cross section, while the rest is practically impermeable.

4.3 PHYSICAL STATE OF THE WATER IN Na-MONTMORILLONITE

While the water in external pores is in free form, the internal or interlamellar water is concluded to be organized and adsorbed, either by forming hydrates of interlamellar cations, which is certainly the case for Ca montmorillonite, or by forming a water lattice that grows directly on the basal planes of the flakes. The latter case, which implies that hydrogen bonds and van der Waals bonds are responsible for the water lattice strength and the mineral/water interaction, fits well with Forslind's concept of water association in montmorillonite gels at temperatures below about 100°C (23) and with Sposito's and Prost's conclusion (24) that at least the first hydrate layer has the form of a strained, significantly deformable ice-like lattice. The low density of the interlamellar water that has been determined experimentally, i.e. about 0.9 t/m^3, is also in support of this model. Forslind's view, as illustrated in Fig 11, is that the crystal structure of montmorillonite at temperatures lower than a certain critical range is equivalent to that forwarded by Edelman & Favejee (EF) and that higher temperatures cause breakdown of the apical tetrahedrons, thus yielding the traditional Hoffman, Endell & Wilm (HEW) structure (cf. Fig 12).

Provided that there actually is a heat-induced transition between the two structural states and that they are real, heating to the critical temperature would bring the silica atoms in an unstable condition by which they would be released and free to move in the interlamellar space. The resulting gradient in concentration of liberated silica would logically cause it to migrate towards the edges of the montmorillonite stacks, where it may become precipitated as suggested earlier in

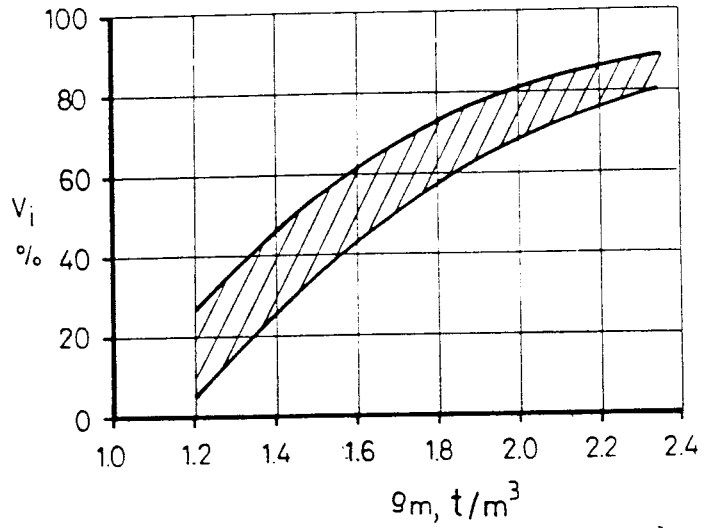

Fig 10. General relationship between bulk density and content of internal water in percent of the total porewater volume of smectite clays (18). The equivalent dry densities are obtained from the expression $\rho_d = (\rho_m - 1)/0.63$

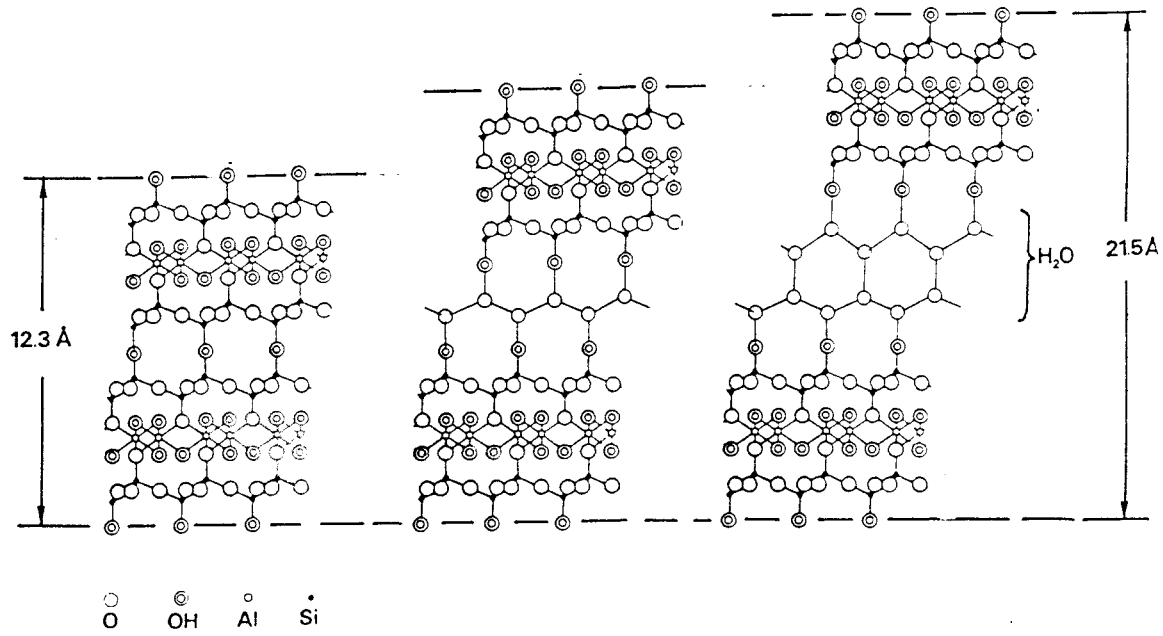

Fig 11. Schematic picture of regular H-bonded water lattices formed between apical OH:s of opposing basal planes in interlamellar space following Forslind's concept

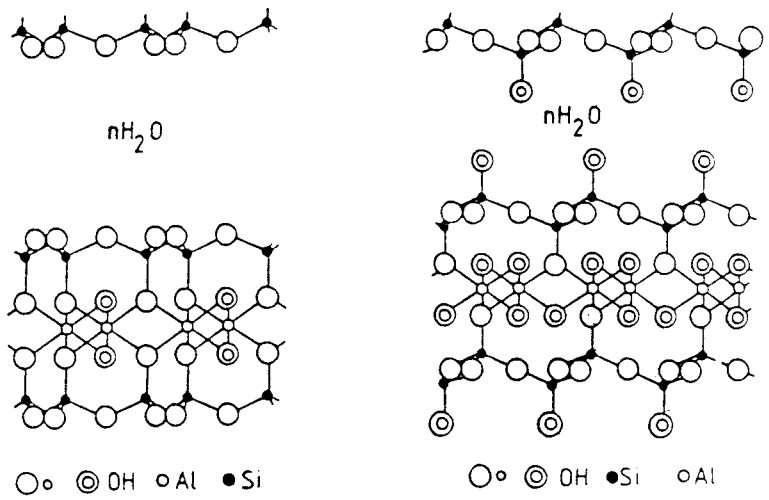

Fig 12. Crystal lattice states of montmorillonite. Left: The Endell/ Hoffman/Wilm structure. Right: The Edelman/Favejee structure

the report (25). The migration of silica would logically take place in connection with collapse of the structure from the 12.5 Å state in Fig 11 to the dehydrated 10 Å state, provided that external compressive forces or dominating attraction forces between neighboring flakes yield contraction of the stacks, and that the migration of silica is associated with expulsion of water formed from the OH:s. The contraction is expected to be largely reversible on cooling as long as no cementation of the flakes has taken place, which would imply that the beidellitization process, yielding free silica, is not associated with a permanent contraction of the stacks of montmorillonite flakes. If there is no silica precipitation, the rheological properties and the perviousness should therefore not be significantly changed after cooling, provided that no other heat-induced microstructural alterations are generated.

4.4 DISCUSSION

4.4.1 Expected influence of heating

Microstructural changes in the form of a decrease or increase in basal spacing are associated with a change in swelling pressure, a drop in swelling pressure imply-

ing that the interaction between adjacent stacks of flakes is diminished if the total volume of the water saturated clay is kept constant. If we imagine a theoretical case where such reduced interaction is due to heat-induced contraction of stacks of montmorillonite flakes and the total volume is kept constant while the excess pore pressure in the heated water is free to dissipate by allowing for drainage, the swelling pressure is expected to drop. Actually, this is equivalent to a drop in preconsolidation pressure of ordinary clays, which means that compression by expulsion of external water will take place if there is an external load and compression is allowed for.

Heat-induced contraction of the stacks resulting from a decreased number of hydrate layers would logically be due to structural breakdown of the organized interlamellar hydrates caused by increased thermal vibrations. Like in the case of freezing, the loss of interlamellar water is assumed to be rapid and to take place more or less stepwise (26). Applying for the moment Forslind's EF-based concept, the basal spacing may be retained at about 12.5 Å at rather high temperatures, a theoretically derived temperature value for complete dehydration and collapse to 10 Å basal spacing being 170-190°C (27). According to the conventional HEW model removal of the last hydrate layer would yield a basal spacing of 10 Å. The difference between the models is fundamental and not until the matter of crystal constitution of montmorillonite has been settled, the true hydration/dehydration mechanisms can be identified.

A primary reason why interlamellar dehydration and collapse of the stacks would take place on heating under constant volume conditions is that the attraction forces that hold the flakes together dominate over the compressive resistance produced by the remaining hydrates. It is quite obvious from the larger "thickness" of the third hydrate than of the second, that the mechanical strength of the latter is significantly higher, the strongest hydrate layer naturally being the first one. Successively higher temperatures are therefore required to make the contraction proceed and considerable, thermally induced disturbance is therefore logically required to yield complete dehydration, which is known to require an effective pressure of about 200 MPa at room temperature. In very general terms the stability of sandwiched thin water films and solids, like those represented by phyllosilicate flakes with interlamellar water, can be explained in terms of mass forces and entropy effects (25). Applying Frenkel's theory (28) one finds that sandwiched systems consisting of very thin silicate flakes separated by equally thin (~10 Å) water films should collapse to form thick solid particles. The reason why

interlamellar water films that are only a few molecules thick still exist at room temperature in hydrophilic clays is the entropy component, the main contribution of which is in the region of small film thicknesses. The general conclusion from this is that colloidal particles may remain attached to each other through extremely thin films of a dispersive medium provided that there is an ordering influence induced by the solid substance, of which montmorillonite gels are typical examples.

Applying Frenkel's views, it is clear that a sufficient increase in temperature inducing thermal motions would yield instability of the water films. Thus, heating to certain critical temperature levels is expected to lead to stepwise contraction of previously expanded montmorillonite stacks.

4.4.2 Influence of pressure

While the effective pressure concept is perfectly valid for non-smectite clays and coarser soils it may be only partly applicable to Na montmorillonite clays. This depends on the physical state of the interlamellar water, which is able to transfer normal stresses across the clay/water stacks. Basically, taking the pressure in the interlamellar water to be equal to the effective pressure and to the swelling pressure, one expects that it is independent of the pressure in the external water, i.e. the porewater pressure. This is supported, in principle, by various experiments but considering the arrangement in Fig 11 and the general conclusion that the interlamellar water is organized and has a lower density than that of free water, it may be believed that very high porewater pressures could yield compression of the interlamellar water and a change in its energy state. The maximum strain that can be absorbed without breaking molecular bonds is relatively large as concluded from the fact that even bonds that are more sensitive to deformation than the hydrogen bond and electrostatic bonds, are only moderately altered by relatively large imposed strain. Thus, the energy state of covalent bonds in molecules like HCN and C_2H_2 is changed by no more than 3-15 % on altering the interatomic distance by 10 % and much less than that on imposing angular changes by as much as 5° (29). Van der Waals forces would be somewhat more sensitive to changes in distance, while hydrogen bonds, which are essentially electrostatic, are less altered by distance changes. We conclude from this that isothermal compression of interlamellar hydrates by a few percent does only involve an insignificant change in energy state of the water molecule lattice at room temperature.

No change in the number of interlamellar hydrates is therefore expected to take place at such a small strain at any particular temperature.

Naturally, larger strain - associated with bulk compression - yields a change in the number of hydrates and swelling pressure as demonstrated by the relationship in Table 1, which is based on common data compiled from earlier SKB research work. This table also illustrates the span in basal spacing and associated variation in swelling pressure for each individual set of hydrate layers. Naturally, there is a variation in the number of hydrate layers at any bulk density, since the distribution of effective stresses is related to the microstructural heterogeneity. At bulk densities lower than about 1.4 t/m3, the number of hydrate layers in the stacks is at maximum, i.e. 3, and macroscopic swelling beyond that state is due to separation of clay stacks caused by double layer interaction as explained by conventional colloid chemistry.

While, at constant temperature and drained conditions, load transfer between adjacent stacks ("effective pressure") controls the basal spacing by yielding expulsion or uptake of interlamellar water (and external water), to yield force equilibrium, the pore pressure exerts isotropic pressure on the internal water films and cannot produce expulsion of such water. Elastic strain is, however, expected as discussed in the preceding text and collapse of the interlamellar water to a denser form, approaching the state of free water, would possibly be expected at very high porewater pressures. It appears, however, that at room temperature the pressure required to cause such changes corresponds to several hundred megapascals (30). At higher temperature the effect may be quite different as outlined in the subsequent chapter.

4.4.3 Combined heating and pressure increase

Experiments (31) have indicated that there is a 50 % drop in swelling pressure on heating of MX 80 bentonite to 90°C under constant volume conditions, which means that although some contraction of the interlamellar space takes place it may not have the form of a drop in the number of interlamellar hydrates at such a temperature change (cf. Table 1). The thermally induced disturbance must cause some weakening of the water lattice by which the attraction forces dominate over the repulsive forces and a certain elastic contraction of the water lattice therefore naturally takes place under confined conditions also when the temperature is raised even moderately above 20°C. Higher temperatures yield stronger thermal

Table 1. Relationship between density, basal spacing and swelling pressure of MX80 Na bentonite at room temperature (dist water)

Bulk density t/m^3	Dry density t/m^3	Swelling pressure MPa	Basal spacing Å	Approximate number of hydrates	
				Forslind/EF	HEW
2.1-2.2	1.75-1.90	20-50	13.7-14.6	1	1-2
2.0-2.1	1.59-1.75	5-20	14.6-16.5	1	2
1.9-2.0	1.42-1.59	2-5	16.5-18.3	1-2	2-3
1.7-1.85	1.08-1.34	0.5-1.5	18.3-19.3	2	3
1.5-1.7	0.79-1.08	0.2-0.5	19.3-23	2-3	3[1)]
1.4-1.5	0.6-0.79	<0.2	23-27	3	3[1)]

1) Assumed maximum expansion

vibrations and a potential to break down the water lattices and they are therefore expected to cause step-wise reduction in the number of hydrates so that force equilibrium is established. Dehydration in combination with bulk compression under external loads naturally takes place under drained conditions, which usually prevail in nature, while loss of interlamellar hydrates to the external water in the voids under constant volume conditions requires a higher internal than external pressure. The thermodynamics involved in this context is under consideration and only preliminary estimates can be made at present. In principle, the attractive forces operating between the flakes and the interlamellar cations create the internal pressure, the external pressure being superimposed on the system. As mentioned previously, external water pressure generates a corresponding additional isotropic internal pressure which yields elastic compression of the interlamellar water. At high temperatures, high porewater pressures can therefore possibly contribute to the compression or cause collaps of the interlamellar water lattices and at the stage of collapse, when the internal pressure is higher than the external water pressure, they help to expell interlamellar water to external voids.

A preliminary concept based on all these considerations would be:

* Moderate heating, i.e. exposure to temperatures lower than 50-60°C, and moderate porewater pressures, are expected to yield mainly

minute elastic contraction of the montmorillonite stacks. Wider interlamellar openings than the average measure at equilibrium may contract on loosing 1 hydrate layer. Not even very high porewater pressures are expected to yield appreciable changes in the physical state of interlamellar water

* Heating to 60-90°C may induce contraction by one hydrate layer in which process high porewater pressures may be a contributing factor

* Heating to about 110°C and low porewater pressures, i.e. lower than the swelling pressure, may yield loss of all but one interlamellar hydrate layer. Increase of the porewater pressure even to very high values is not expected to yield complete dehydration at least not as long as the pressure is less than a few tens of megapascals

* Heating to more than 150°C may cause loss of all interlamellar hydrates of the HEW model, while it would be logical to assume that the more strongly established system with apical tetrahedrons of the EF model could still resist breakdown and thus yield 12.5 Å basal spacing, i.e. with no interlamellar hydrates

* Hydrate water leaving interlamellar space on heating, possibly assisted by high porewater pressure, enters the void system and transforms to slightly denser external water. This yields a slight drop in porewater pressure at heating under constant volume conditions, while consolidation and return to the ambient piezometric conditions occurs under drained conditions, i.e. in nature

* At heating under constant volume conditions, the rather high elastic compressibility of the interlamellar hydrates partly compensates for the tendency of increase in volume of the external water and it thereby moderates the build-up of high porewater pressures. At high bulk densities, i.e. when the amount of interlamellar water exceeds that of external water, this pressure-reducing effect should be substantial.

4.4.4 Comment

The hypothesis that heating to 50-60°C will change the number of hydrate layers only of a small fraction of the interlamellar water films and that such a change is expected to be very moderate also in the temperature range 60-90°C, is supported by NMR experiments using MX 80Na bentonite (30). Thus, the proton relaxation properties in terms of T_2 was found to increase by about 30 % on increasing the temperature from room temperature to 72°C (Fig 13), which exactly corresponds to the drop in viscosity of free water on heating to the same level (26-72°C). The change in relaxation time may hence be related entirely to the increased thermal vibrations in the external water. This matter is presently being looked into in detail.

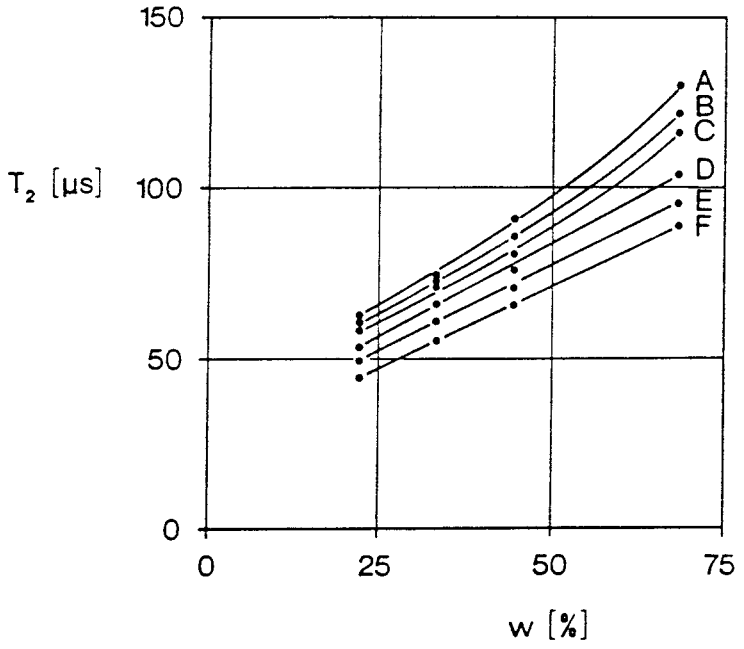

Fig 13. Proton T2-relaxation time in MX-80 with distilled water. A:72°C, B:65°C, C:54°C, D:38°C, E:26°C, F:13.4°C (31)

4.4.5 Conclusions

Microstructural changes are expected on heating, the major effect being a contraction of initially expanded stacks. This contraction is assumed to be very moderate at heating to temperatures lower than 60-90°C even at extreme porewater pres-

sures, while it should be significant at temperatures around 100°C, at which dehydration to 1 hydrate layer may take place. The influence of the porewater pressure is probably not very important. At around 150°C complete dehydration may take place and this stage is almost certainly reached at about 200°C. At these higher temperatures very high porewater pressures should help to maximize the contraction of the stacks.

On release of temperature and porewater pressure, rehydration to the original state is expected unless cementation by precipitation of dissolved substances has taken place or permanent heat/pressure-induced collapse of the stacks, resulting in 10 Å-12.5 Å minerals, has occurred. If hydrothermal tests on Na montmorillonite are conducted at the temperature levels mentioned, varying the porewater pressure, information would be obtained on whether permanent microstructural changes are induced by heat treatment. Identification would be possible by use of electron microscopy as well as X-ray diffraction analysis.

A combination of the investigations concerning silica precipitations mentioned in Chapter 3 with the presently suggested additional study would thus be fruitful and the hydrothermal test series that formed part of the present project confirmed this.

5 EXPERIMENTAL

5.1 SCOPE OF TESTS

The purpose of the study was to develop equipment for conducting heating tests of soft and dense Na montmorillonite clay, and to find suitable methods for analyzing the reacted clay, as well as to run test series at different porewater pressures and temperatures. The duration of the tests was set at 1 week to 1 year.

5.2 TEST CONDITIONS

5.2.1 General

More specifically, the conditions for the testing had to be chosen so as to yield conclusions with respect to the following two major questions:

1 Is silica released and precipitated non-congruently on heating to 100-200°C and subsequent cooling to room temperature?

2 Does heating to various temperatures in the interval 60-200°C, and subsequent cooling to room temperature yield microstructural changes?

The first-mentioned issue was expected to give information not only of the mechanisms in silica cementation but also to shed some light on whether there is a critical temperature for release of silica, and thereby if there is a transition from a "low-temperature" (EF) to a "high-temperature" (HEW) crystal state of montmorillonite, possibly in relation with the transformation of montmorillonite to beidellite. A natural way of running tests of this kind is to use autoclaves, the most important test criterion being to use closed systems for the retainment of the porewater throughout the respective test.

The second matter would require a large temperature span and different porewater pressure levels, which would call for at least half a dozen autoclaves. Considering the pilot character of the study, a simpler and cheaper variety was choosen at the planning in early 1986. It involved construction of closed cells of different size designed so as to yield different water pressure levels at certain selected temperatures. They are described in detail in Chapter 5.2. The experimental work

started in mid 1986 with the development of suitable hydrothermal cells, and the larger part of the initially planned tests was finished in late 1987. The remaining ones were finished in May 1988.

5.2.2 Hydrothermal treatment

5.2.2.1 Preparation of clay material with special respect to impurities

The chemical composition of the water in interaggregate voids of natural bentonite deposits of sedimentary origin is primarily dependent on the composition of the sea or estuary in which the clay was formed. Usually, the content of dissolved silica in such water is less than the solubility - except perhaps where tropical rivers are discharged in the sea - which means that the silica concentration in the porewater at early stages of the compaction in nature is low. Precipitation of this substance would thus not take place in the pores of a clay sediment unless the concentration is increased to 20-30 ppm, when quartz is formed, while amorphous silica becomes precipitated at a somewhat higher concentration. Actually, however, hydrated amorphous silica gels may be formed first as concluded from various investigations of clay soil material, indicating that 1-10 Å amorphous coatings of clay minerals are produced by hydrolysis as a result of weathering (32). Such hydrous silica and aluminosilicate gels are expected to occur in young formations, while they may well have altered to opal, and to the crystalline forms quartz and cristobalite in old beds with no groundwater percolation and stagnant porewater. It was therefore clear that tests on standard MX-80 or any other commercial bentonite would not be suitable since severe difficulties would then appear in distinguishing original and heat-induced enriched silica. A pure smectite clay used as an international reference substance, (SWY 1) was therefore selected but already the first few electron microscopy tests showed that it also has a certain content of very small dispersed quartz and iron bodies, most of which could be removed by centrifugation. Additional analyses demonstrated that electrophoretic treatment, applying necessary buffering to avoid too low pH, and centrifugation, yield a perfectly clean montmorillonite material. Since such treatment turned out to be extremely time-consuming only centrifugation was applied in the preparation of samples for the hydrothermal treatment.

5.2.2.2 Clay material

Clay originating from Crook County (Newcastle Formation), Wyoming, USA, was used for the experiments. It is termed SWY-1 and was purchased from the company Norsk Hydro, Norway, according to which the chemical composition is as follows (%):

SiO_2:69.2, Al_2O_3:19.6, TiO_2:0.090, Fe_2O_3:3.35,
FeO:0.32, MnO:0.006, MgO:3.05, CaO:1.68, Na_2O:1.53,
K_2O:0.53, P_2O_5:0.049, S:0.05, F:0.111

The montmorillonite content of the minus 2 µm fraction of this clay is at least 90 %, the main accessory minerals being quartz and carbonates. The larger part of the iron is in octahedral lattice positions, while the rest is in the form of dense iron micronodules. In the present study particles with a Stoke diameter larger than 1.0 µm were removed through a sedimentation process, by which the montmorillonite content ought to have risen to only slightly less than 100 %.

5.2.2.3 Preparation of clay gels

Clay gels with a dry density of 0.48 and 1.59 g/cm^3 were prepared by adding distilled water to air-dry SWY-1 Na montmorillonite powder at room temperature. The gels were formed in the cells in different ways, some of them being filled with thin, alternating layers of clay powder and distilled water, the amounts calculated so as to yield almost complete saturation on heating and homogenization. A set of bigger deformable cells were filled with well fitting samples of clay that had been saturated in swelling pressure oedometers.

5.2.2.4 Hydrothermal cells

Two major types of gold-plated cells were developed, a smaller 0.4 ml version of brass used for the sandwiched clay-water mixtures, and a larger 4.6 ml type of copper into which trimmed, well fitting cylinders of largely water saturated clay were inserted (Fig 14). The goal of keeping the porewater pressure relatively low, i.e. at approximately the vapor pressure, in one series of tests, and high in a parallel series, was achieved by allowing for an initial degree of saturation that was in the range of 90 % to 98 % depending on the ultimate density and temperature. For the larger cells complete saturation was expected at a temperature of

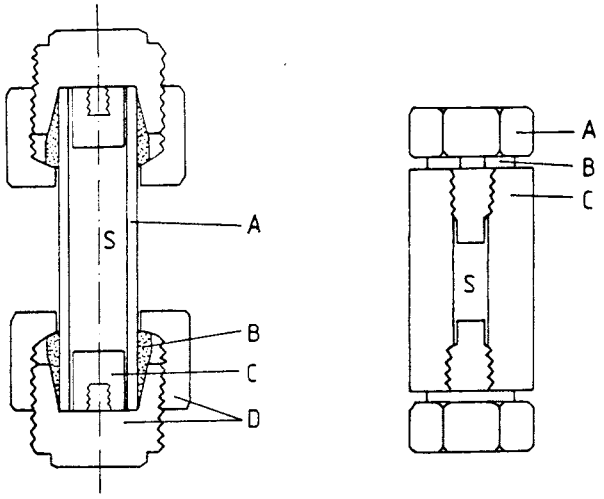

Fig 14. Hydrothermal cells. Left: 4.6 ml copper tube (A) equipped with self-sealing wedge (B) and copper lids (C). D is steel nut components for closure. Right: 0.4 ml brass tube (C) with brass bolts (A) for closure and copper ring for sealing

about 50-70°C. Additional heating would theoretically produce a porewater over-pressure of about 100 MPa per additional 100°C if the cells had been perfectly rigid. The copper tubes were designed so as to allow for slight plastic deformation and since their end caps had to be somewhat displaced axially to yield effective sealing, the net deformation was estimated to yield a porewater overpressure of 20-40 MPa at 200°C. The corresponding increase in diameter was expected to be less than 2 %, which the cells were assumed to sustain as concluded from the stress/strain properties of the copper material. This was also found to be the case but the considerably larger strain caused by heating to 250°C in three trial tests gave cell failure, indicating that the degree of water saturation was as expected in the larger cells. Measurement of the diameters of the cells in the course of the tests turned out to show that radial expansion was in the range of 1-2 % and the evaluated porewater pressures were therefore higher than the expected ones. Thus, the water pressure in the copper cells at 200°C were concluded to have been about 40-70 MPa in samples with a dry density of 0.48 g/cm^3 and 20-40 MPa at a dry density of 1.59 g/cm^3. At lower temperatures the pressure was correspondingly lower, but even at 105°C it amounted to 6-12 MPa in the copper cells. The aim of running one series of tests at low and one at high porewater pressures was thus arrived at.

5.2.2.5 Test program

Initially, the test program comprised only a limited number of experiments but it was expanded in the course of the study in order to get a more detailed picture of the temperature influence. The test data are compiled in Tables 2 and 3, referring to "low" and "high" porewater pressures, respectively. The total number of tests was 31.

Certain samples were soaked with 3.7 M KCl solution under confined conditions for at least 2 months after the heat treatment in order to find out whether illite would be formed under the prevailing conditions.

5.3 ANALYSES

5.3.1 XRD swelling tests

The expandability of the clay material was investigated by measuring the basal spacing of specimens extracted from the cells. The preparation included drying and grinding and exposing the powder to a relative humidity of 40 to 100 % in the goniometer chamber. Ultrasonic dispersion was not applied.

5.3.2 XRD mineral "finger prints"

XRD tests were made of reference samples as well as of heated samples with and without ethylene glycol treatment. The investigation was conducted by the Swedish Geological Survey. Ultrasonic dispersion was made in deionized water as a first step in the preparation of air-dry and EG-treated specimens.

The KCl-soaked material was only gently stirred in order not to create complete disintegration of collapsed stacks.

5.3.3 Rheological properties

Undisturbed samples were extruded from the cells for uniaxial compression tests. After the hydrothermal treatment the cells had been stored at room temperature, yielding zero water pressure for several weeks after the heat treatment, which allowed for complete redistribution of "external" water from larger pores back to

Table 2. Test program for "low" porewater pressures. LD represents "low density" and HD "high density" tests. u denotes estimated porewater pressure

Test no	u MPa	ρ_d g/cm^3	T °C	t years	Tests					Remark
					TEM	SEM	XRD nat	XRD KCl*	Rheo	
LD1	0	0.48	20		x					Ref
LD2	0	0.48	20		x	x	x	x	x	"
LD3	0	0.48	20		x	x	x	x	x	"
LD4	5	0.48	225	0.05	x					
LD5	3	0.48	225	0.05	x					Not sat
LD6	0.5	0.48	150	0.3	x					"
LD7	0.5	0.48	150	0.5	x		x			
LD8	0.5	0.48	150	1.0	x	x			x	
LD9	0.1	0.48	105	0.5	x			x		
LD10	0.1	0.48	105	1.0	x	x			x	
LD11	~0.1	0.48	60	1.0					x	
HD1	0	1.59	20		x	x			x	Ref
HD2	0	1.59	20		x	x			x	"
HD3	0.5	1.59	150	1.0	x	x				
HD4	0.1	1.59	105	1.0	x	x				
HD5	~0.1	1.59	60	1.0	x	x			x	

x Denotes that the respective test has been conducted
* Denotes that the sample was saturated with KCl solution after the heat treatment

interlamellar positions if permanent contraction of the stacks had not been caused.

Table 3. Test program for "high" porewater pressures. LD represents "low density" and HD "high density" tests. u denotes estimated porewater pressure

Test no	u MPa	ρ_d g/cm3	T °C	t years	Tests					Remark
					TEM	SEM	XRD nat	XRD KCl*	Rheo	
LD12	>70	0.48	250							Cell broken
LD13	>70	0.48	250							"
LD14	40-70	0.48	200	0.1	x	x	x		x	
LD15	40-70	0.48	200	0.5			x	x	x	
LD16	40-70	0.48	200	1.0						Not sat
HD8	>70	1.59	250							Cell broken
HD9	20-40	1.59	200	0.02	x				x	STEM**
HD10	20-40	1.59	200	0.1	x				x	"
HD11	20-40	1.59	200	0.5	x	x		x	x	
HD12	12-25	1.59	160	0.02	x				x	STEM**
HD13	12-25	1.59	160	0.1	x				x	"
HD14	9-18	1.59	130	0.02	x				x	"
HD15	6-12	1.59	130	0.1	x				x	"
HD16	6-12	1.59	105	0.02	x				x	"
HD17	6-12	1.59	105	0.1	x				x	"

x Denotes that the respective test has been conducted
* Denotes that the sample was saturated with KCl solution after the heat treatment
** Includes EDX

Extreme care was taken to avoid mechanical disturbance in the preparation of samples and a precision load device with electronic strain measurement was used for maximum resolution at the recording of the stress/strain behavior. The compression took place in humid atmosphere to eliminate evaporation from the clay in the 25 to 50 minutes long tests.

5.3.4 Electron microscopy

Transmission electron microscopy of ultramicrotomed (500-1000 Å) sections of resin-embedded clay was used for investigating whether the heat treatment had altered the microstructure and produced precipitates. The resolution power, which was better than 10 Å using the available JEOL 100 TEM microscope, allowed for a safe identification of possible alterations, the problem being to avoid artefacts by applying proper preparation techniques.

High voltage microscopy of undisturbed smectite clay in water saturated and resin-bedded forms has shown that the microstructure may be only insignificant affected by certain resin embedding techniques (33). The present study was made by applying two particularly suitable methods one of which involves replacement of the porewater by ethylene alcohol and propylene oxide which are, in turn, exchanged by Spurr resin that is polymerized at about 50°C. The replacements take place through diffusion, which makes the procedure very time-consuming, which is the case also for the other procedure that involves replacement of the porewater by ethylene alcohole of successively increased concentration and then exchanging the alcohole by butyl/methyl methacrylate, finally polymerizing the embedding monomer mixture at 60°C. Both techniques yielded similar results. The dense samples had to be freeze-dried before soaking them with the embedding substance. All samples were confined in hollow filters which were submerged in the monomer mixture for a few weeks to allow for complete saturation.

SEM low voltage microscopy of freeze-dried uncoated specimens was also applied for investigation of the surface character of the stacks of flakes and for the identification of possible precipitations caused by the heat treatment. The resolution power of the Philips SEM 515 instrument is about 50 Å at best.

STEM microscopy was applied for microstructural imaging and for chemical analysis of ultramicrotomed specimens, the instrument being a JEOL 100 microscope equipped with a Kevex 8000 EDX facility. It belongs to the Geological Depart-

ment of Texas Tech University at Lubbock, Texas, where this study was conducted. An extended study (HD9-HD17) was conducted at the Dept of Physics and Measurements, University of Linköping, using a Philips EM 400 T with a Link 10000 analyzer.

5.4 TEST RESULTS

5.4.1 XRD swelling tests

The general conclusion is that the XRD spectra of heated samples differ insignificantly from those of unheated reference material. Thus, neither the shape or height of the low angle peaks nor the basal spacing of hydrated and glycolated specimens were substantially changed even in samples that had been heated to 200°C (Table 4). It is possible, however, that heating to this temperature still causes a change in expandability that is not revealed by XRD in its common form. Thus, weak cementation bonds, such as those produced by slight silica precipitation, may be fractured by the drying and grinding procedures. A second possiblity is that limited swelling, i.e. to about 19 Å, may well take place also of stacks consisting of flakes that are fixed at the edges by "spotwelded" silica precipitations, while free swelling and spontaneous disintegration at submersion in water would be largely prevented. It may also be that a sufficient amount of flakes are free to move and yield standard XRD patterns, masking even significant edge fixation of most of the flakes.

Table 4. Basal spacing of unheated and heated SWY-1 clay (Å)

RH, %	Unheated	Heated to 200°C
30-40	11.1	11.1
50-60	12.7	12.6
80	14.7	14.7
90	15.8	-
100	18.8	18.8

5.4.2 XRD finger printing

5.4.2.1 Clay extracted from cells

The reference and heated materials in untreated form showed different reflection patterns, the high intensity 001 peak being in the interval 12.4 to 14 Å depending on the RH conditions. The most characteristic measure of possible mineral alterations was assumed to be illustrated by the ethylene glycol runs and careful comparison was made of all EG diffractograms. Fig 15 shows representative XRD graphs, which demonstrate that the intensity actually increased with temperature while the spacing appeared to be larger (17.3 Å) for the 200°C sample than for the 150°C and reference samples (16.7 Å). One finds that the latter two gave almost identical patterns while the bump in the range of $2\theta° = 6\text{-}10$ suggests formation of 10 Å-type minerals or permanent collapse of a certain small fraction of the interlamellar space.

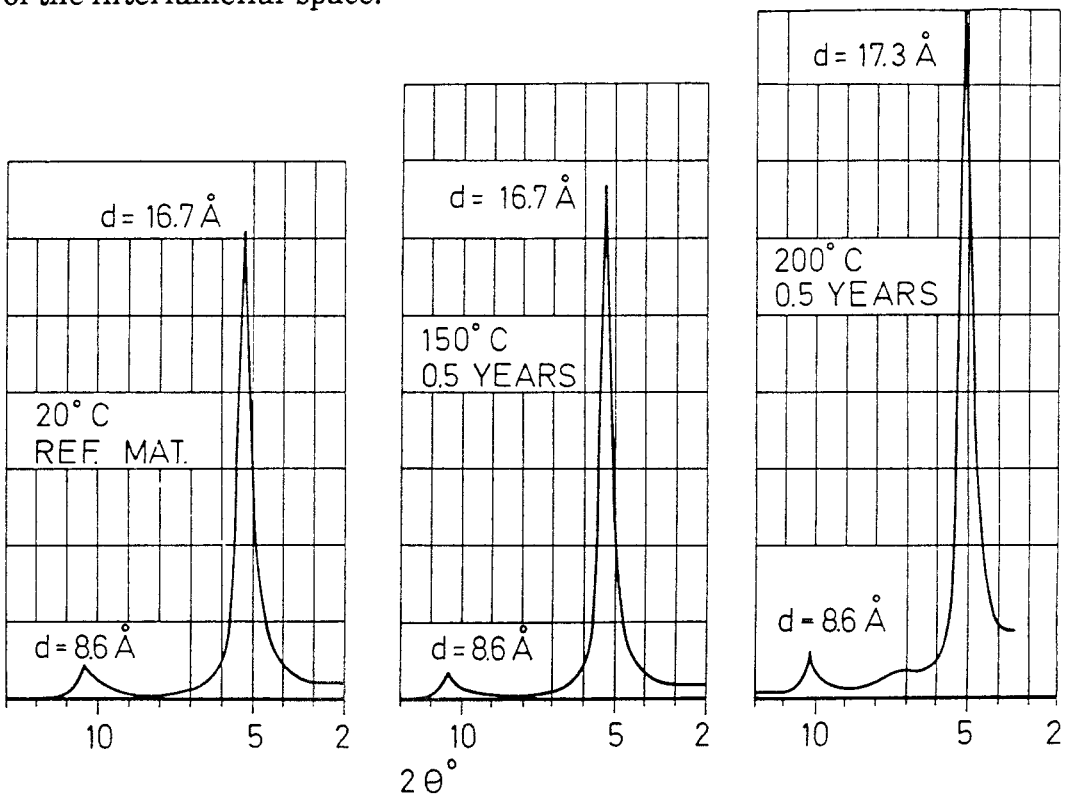

Fig 15. Rectified XRD patterns of EG-treated clay samples. The samples were obtained from Tests LD1 (ref), LD7 (150°C), and LD15 (200°C)

The enhanced intensity of the 001 reflections at increased temperature indicates improved, group-wise orientation of the flakes. The tendency of 10 Å mineral formation at 200°C may be apparent only, since complete dehydration and break-

down of possibly existing apical tetrahedrons without rehydration on exposure to humid air - possibly due to cementation effects or formation of brammalite - would yield a lattice with 001 reflections of approximately 10 Å.

5.4.2.2 Clay soaked with KCl

One reference and a few heat-treated samples were transferred to porous cells which were submerged in 3.7 M KCl solution for at least 2 months by which possibly beidelliticized material was expected to take up potassium and transform to illite. Fig 16, showing normalized diffractograms which offer direct comparison, gives characteristic EG patterns from which we conclude that the reference sample (LD2) was characterized by random orientation of stacks and that heat treatment at 105°C of the soft clay (LD9) caused considerable improvement in this respect. The degree of orientation was assumed to be further enhanced by heating at 200°C (LD15) as suggested by the corresponding development of Na montmorillonite in Fig 15. However, the opposite behavior was observed, the very broad 15.8 peak indicating a first stage in the formation of mixed-layer assemblages with a minor illite content.

The diagram referring to the dense montmorillonite sample heated to 200°C (HD11) shows the rather good orientation that is expected for dense smectite clays, and less illitization than in the soft clay. A rough estimate is that the soft 200°C sample may have contained about 10 % of 10 Å minerals, while the corresponding content of the dense clay cannot have exceeded a few percent, i.e. about the same amount of 10 Å minerals as the Na montmorillonite heated to 200°C (cf. Fig 15). This may indicate that the 10 Å minerals in the KCl-soaked dense clay that had been heated to 200°C were not illite but permanently collapsed groups of flakes.

5.4.3 Rheological properties

The clay samples were carefully extruded from the cells and applied in the loading device for uniaxial compression. Extreme care was taken to avoid mechanical disturbance in the preparation of specimens for the tests, at which the load was applied stepwise and the compression measured by use of an electronic strain gauge. The tests were conducted in humid atmosphere in order to eliminate evaporation from the clay in the 25 to 50 minutes long experiments.

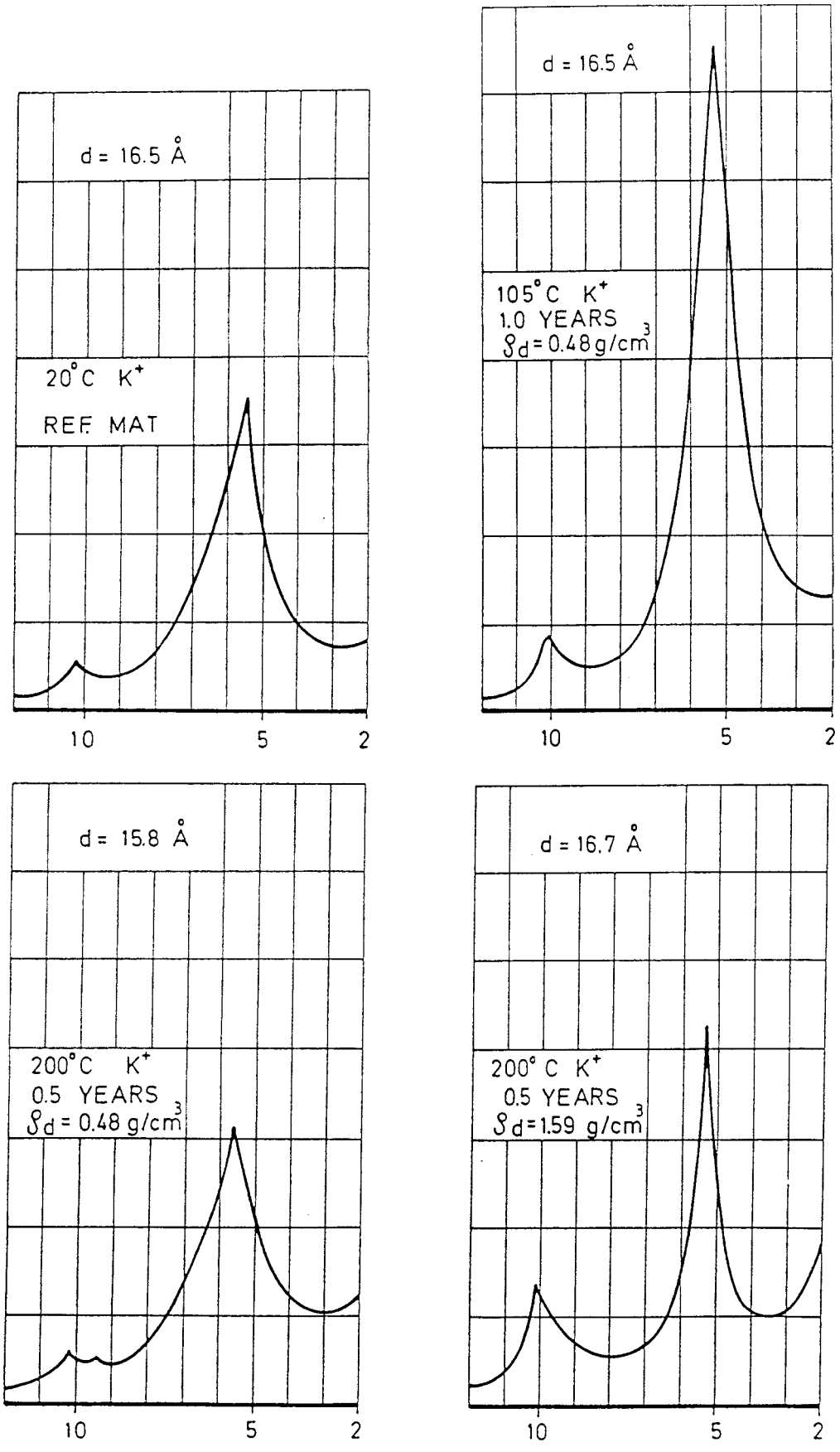

Fig 16. Rectified XRD EG diagrams of KCl-soaked SWY-1 samples pre-heated to different temperatures for long periods of time. The figures on the horizontal scale refer to 2θ°

The upper diagram in Fig 17 demonstrates that the compressive strength of the dense clay heated to 200°C for 0.5 years (HD11) was almost three times higher than that of the unheated reference material (HD1), and that the deformation modulus of the latter was considerably lower. This finding is in agreement with the conclusions from the tests on soft bentonite gels. The soft reference clay, which had matured for two months in the closed cell (LD3), and the samples heated to 105-150°C for 1 year (LD10 and LD8, respectively) and to 200°C for 0.5 year (LD15), gave clearly different unconfined compression strengths. It turned out to be increased by about 30 % for the sample heated to 105°C, and by 70 % for the 150 and 200°C samples. However, the diagram shows that the creep properties were practically the same for the unheated material and for the samples heated to 105 and 150°C, while a significantly stiffer behavior characterized the 200°C sample.

We conclude from this investigation that strengthening is obvious already at about 100°C and that it becomes significant at 150°C. The largely altered rheological properties at 200°C indicate that a second strengthening process took place and that it may well be associated with a significant heat-induced release of silica, which became precipitated to form cementing bonds on subsequent cooling. Assuming that such strengthening actually took place it was expected that the short-term tests HD9 and 10, and HD 12-17 would give evidence of whether the release and migration of silica is an Arrhenius-type process or a mechanism that is triggered by a critical temperature, like the theoretically possible conversion of montmorillonite from the EF to the HEW state. Thus, tests HD 9, 12, 14 and 16, which lasted for 1 week only, would yield a much lower strength increase than the about 1 month long tests HD 10, 13, 15 and 17 if the first-mentioned process applies. Similarly, the ultimate strength value of the 200°C-sample in Fig 17, i.e. 2.9 MPa, would be expected to exceed that of the short-term tests HD 9 and 10 very much.

Fig 18 clearly demonstrates that heating to 105 and 130°C of dense clay specimens gave almost the same strength, which appears to be only slightly higher for the 0.1 year treatment than for the 0.02 year treatment. Heating to 160 and 200°C is concluded to give approximately the same strength independently of the duration of the treatment as suggested by the diagrams in this figure and in Fig 17. We are thus inclined to believe that the significant strength increase and stiffer behavior at elevated temperature is related to chemical alteration at a certain critical temperature level, i.e. about 150-160°C, a probable mechanism being the

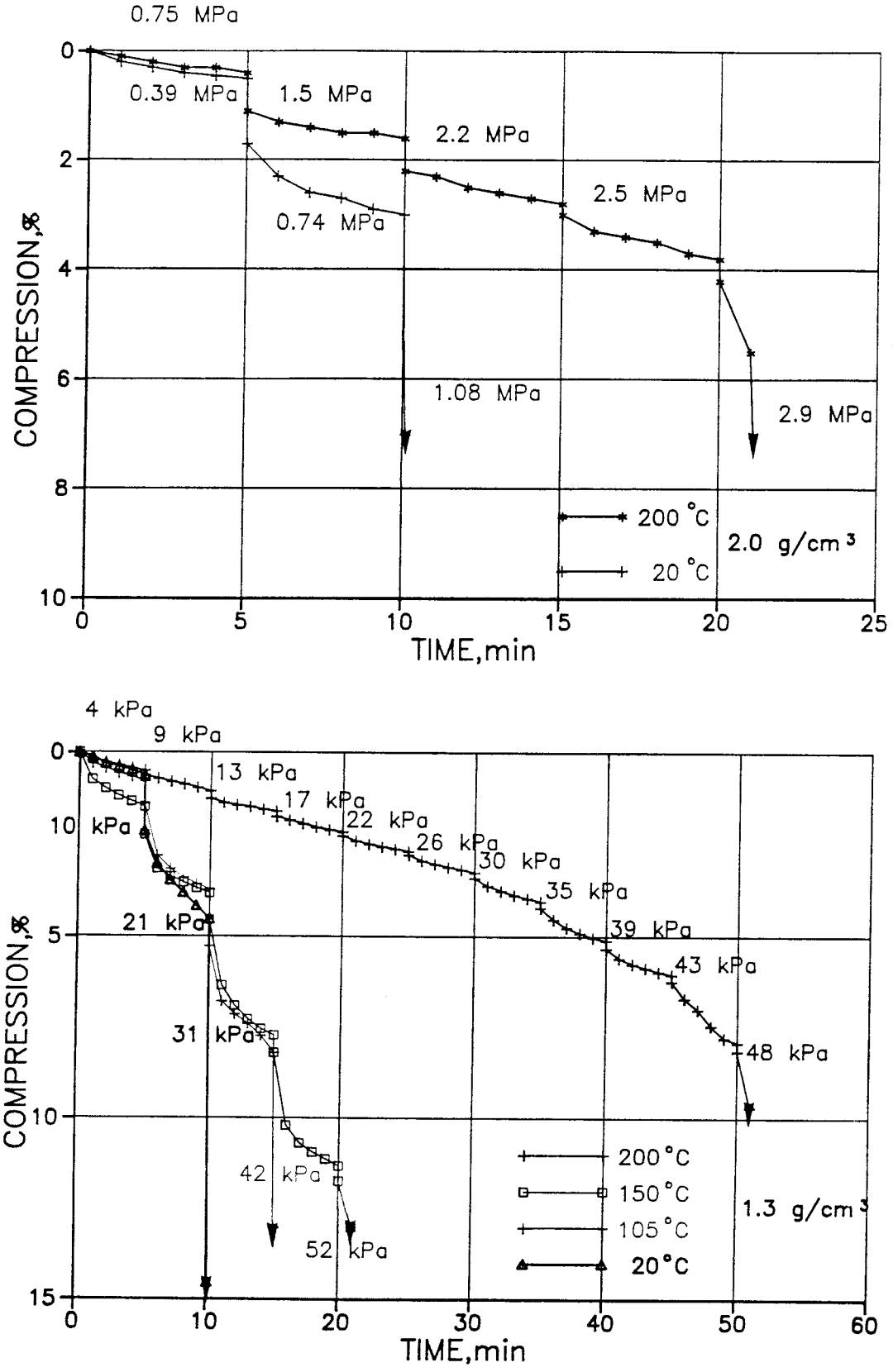

Fig 17. Unconfined compression tests of SWY-1 clay heated for 0.5 years. Upper: high density ($\rho_d = 1.59$ g/cm^3). Lower: Low density after heating to different temperatures ($\rho_d = 0.48$ g/cm^3).

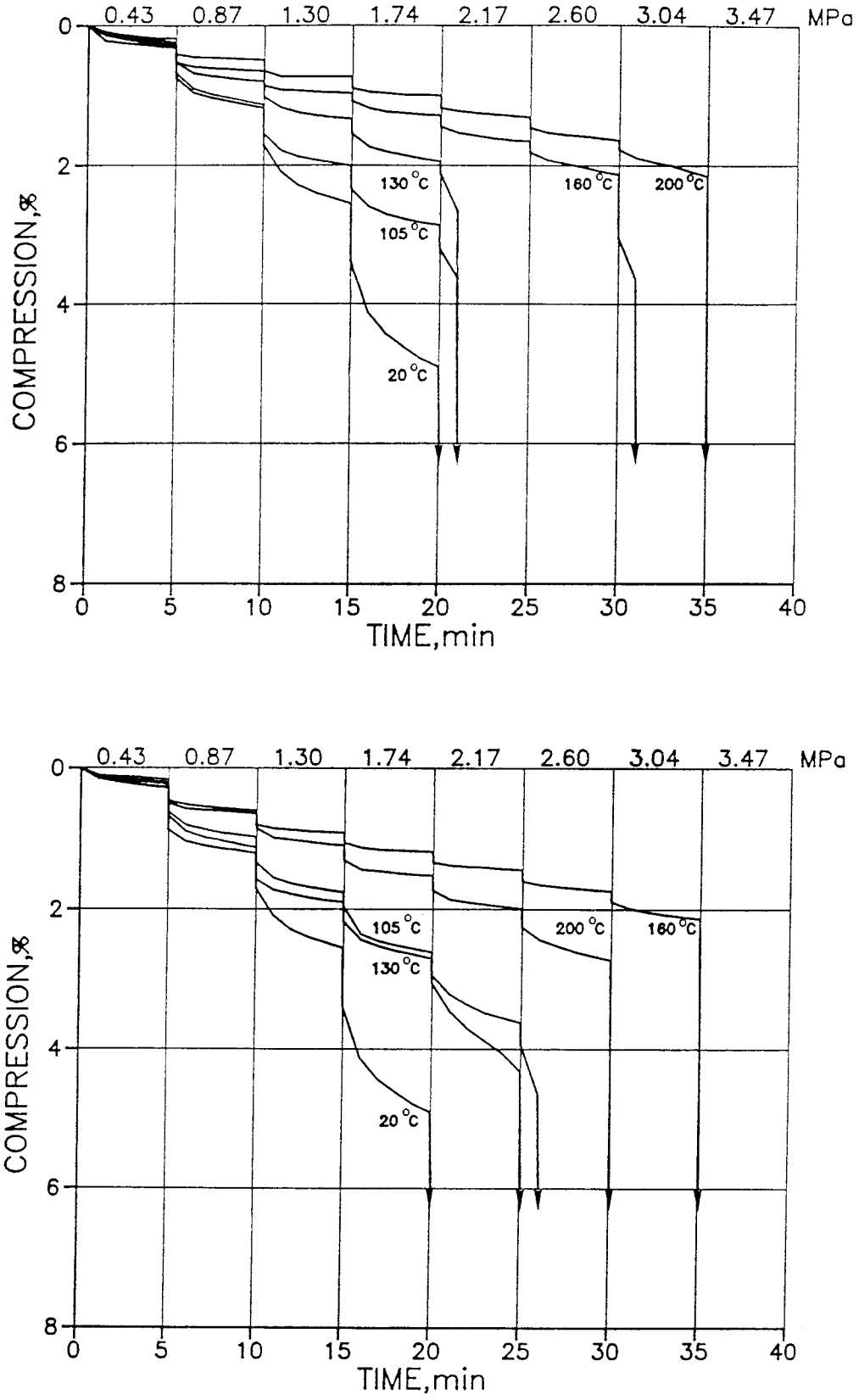

Fig 18. Unconfined compression tests of SWY-1 clay after hydrothermal treatment of short duration (ρ_d 1.59 g/cm^3). Upper: 0.02 year; Lower: 0.1 year

aforementioned EF → HEW conversion associated with release/precipitation of silica.

5.4.4 Microscopy

5.4.4.1 General

The electron microscopy was very comprehensive and yielded a large number of interesting results. Only major findings are reported here.

5.4.4.2 Unheated soft reference clay

The soft reference material exhibited the characteristic features of Na montmorillonite gels in TEM micrographs, i.e. interwoven stacks of parallel, equally oriented flakes, leaving several thousand Å wide voids between the stacks (Fig. 19). This shows that the applied embedding technique had not caused substantial contraction of the fluffy, expanded units. The unheated clay was found to contain a small number of dense agglomerates of nodules with a size ranging from about 0.1 to 0.5 µm. Electron diffraction analysis demonstrated that almost all of these objects were crystalline quartz, some very small Fe-rich particles being present as well (Fig. 20).

5.4.4.3 Heated, water saturated soft clay

The TEM investigation showed that the large majority of the micrographs of all the heated samples showed the same major microstructural patterns as the unheated clay but there was a syneresis-like tendency of the flakes to become more densely grouped, yielding thicker, continuous stacks of flakes separated by larger voids particularly in samples heated to 200-225°C (Fig. 21). These samples had a much higher frequency of agglomerates of dense particles than the unheated clay and they were also much larger, the size generally exceeding the maximum Stoke diameter of the virgin clay material (Fig. 22).

Electron diffraction analysis gave evidence of amorphous silica formed on primary quartz bodies in these large agglomerates and of cristobalite crystals in the agglomerates and on montmorillonite stacks. Both types of precipitates were

Fig. 19 Typical TEM micrographs of unheated SWY-1 clay (ρ_d = 0.48 g/cm^3). The scale is 0.1 µm

assumed to stem from silica that was released from tetrahedral positions of the montmorillonite lattice on heating.

Part of the identified amorphous silica, which was estimated to form about 1 % of the total solid mass, may have been precipitated from the porewater solution in the course of the clay preparation for the microscopy, while some of the cristobalite must have been formed under the hydrothermal test conditions. Thus, at least part of the silica compounds are assumed to have remained dissolved until alcohole and resin replaced the water. These substances diffused rapidly in larger voids and may have displaced some of the silica in the pore system until its concentration finally became so low in the alcohole or resin-rich voids that signifi-

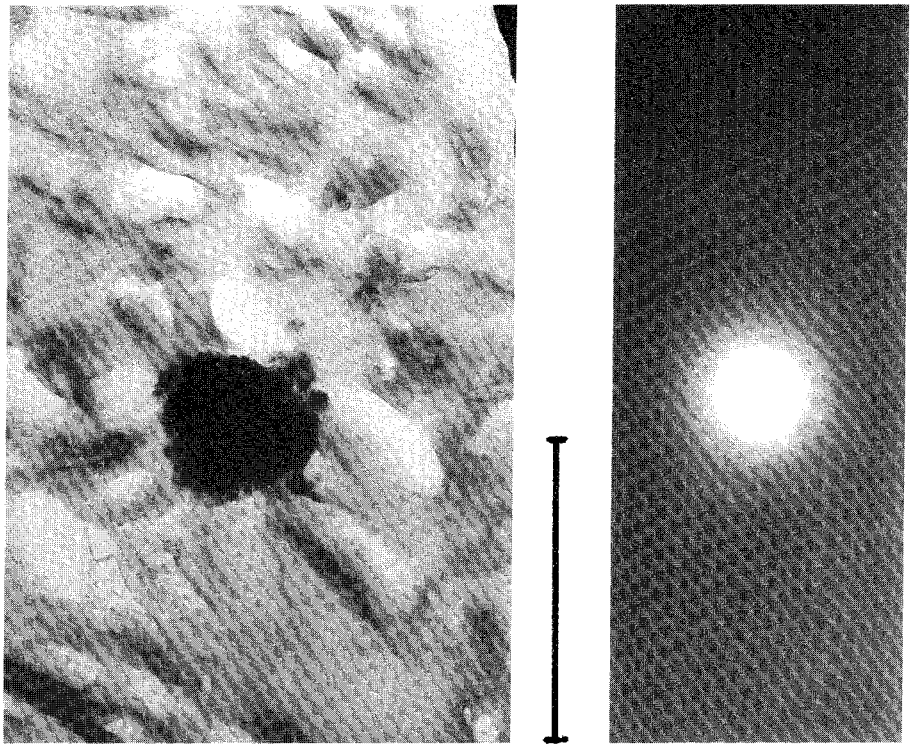

Fig 20. TEM-picture of unheated SWY-1 clay (ρ_d= 0.48 g/cm^3) showing electron-dense agglomerates consisting of very small crystalline nodules in a montmorillonite matrix consisting of an interwoven system of expanded stacks. The scale is 2 µm

cant precipitation occurred. The location of the identified precipitates may therefore be quite different from where the dissolution actually took place.

5.4.4.4 Vapor-treated soft clay

The micrographs of the non-saturated clay in which part of the void system had contained vapor at 225°C and 3 MPa pressure (Test LD5), clearly showed contraction of the montmorillonite stacks (Fig 23). This effect was much stronger than in the saturated clay and it may have had a significant impact on both silica precipitation and rheology, as discussed later in the paper. The degree of water saturation, i.e. the fraction of the pore volume that was filled with water, was approximately 75 %.

5.4.4.5 Dense clay

A dense system of stacks, consisting of aligned montmorillonite flakes and forming interwoven branches of the clay particle network, was found to be the most characteristic feature of the reference clay as observed by TEM and SEM. TEM

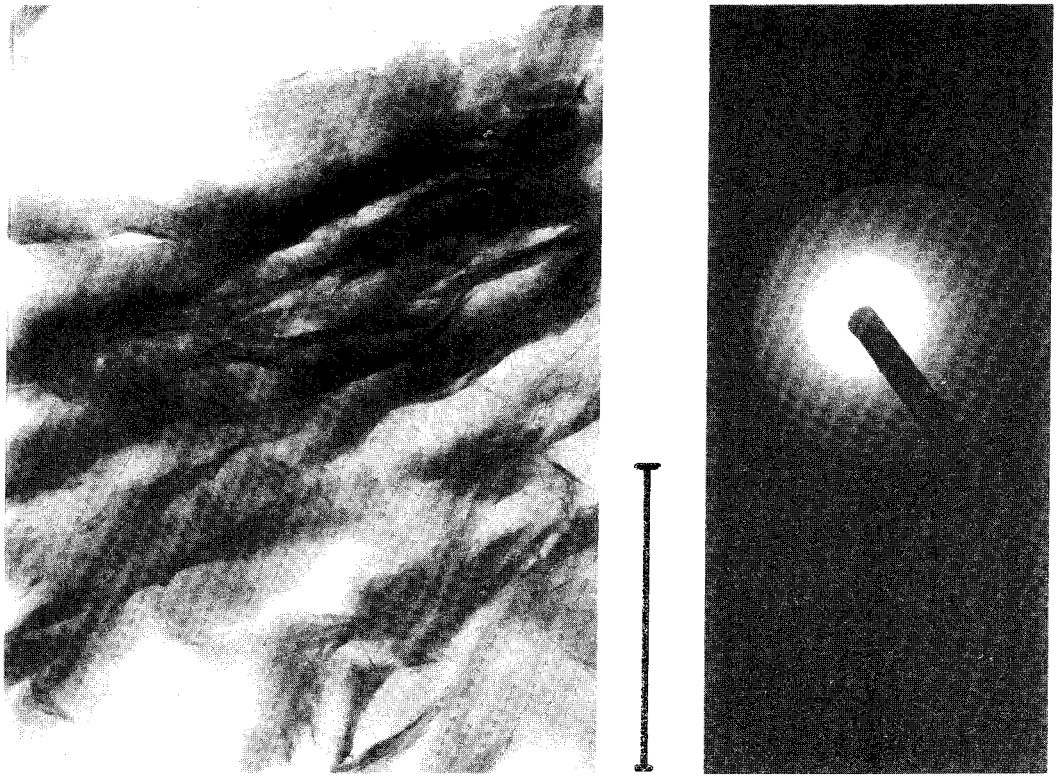

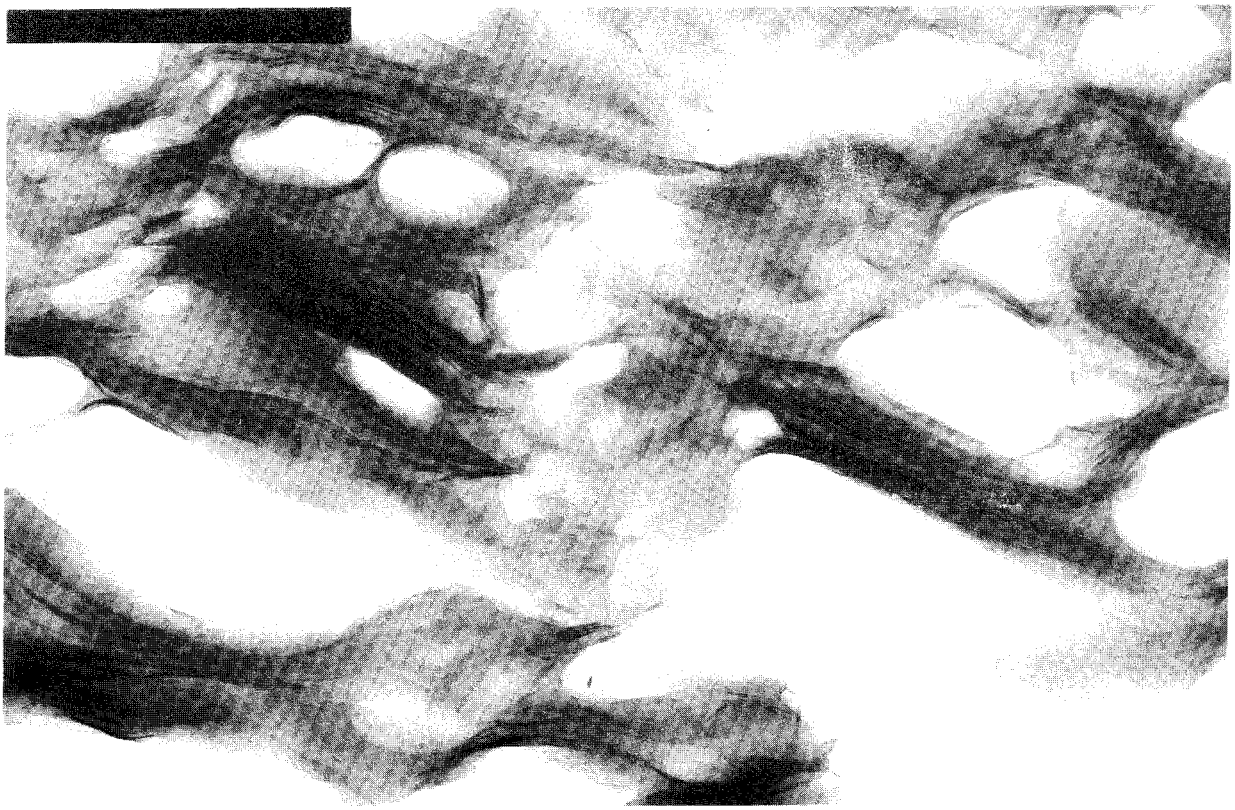

Fig 21. Typical TEM pictures of soft clay heated to 225°C for densely grouped, thicker "branches" of flakes ("syneresis"). The scale is 2 µm

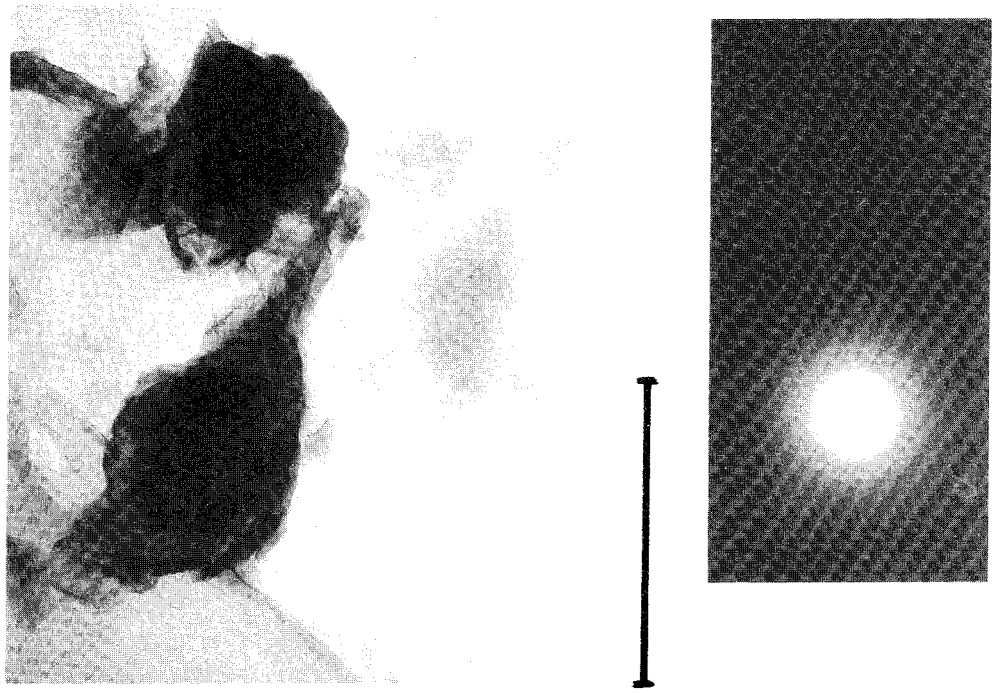

Fig 22. TEM picture showing large non-crystalline precipitations in soft clay heated to 225°C, the scale being 2 µm. Notice the interaction between the clay particle network and the large bodies are presumably precipitations.

pictures of all the heated clays exhibited more condensed network branches but no significant difference in the general microstructural appearance (Fig 24). However, SEM pictures clearly demonstrated that the surface of the stacks was much smoother in the hydrothermally treated clay, indicating collapse of the interlamellar hydrates on heating (Fig 25). This effect, which was observed even for the 105°C sample and appeared to be approximately proportional to the applied temperature, did not seem to be time-dependent.

5.4.4.6 Identification of silica precipitations

TEM-based search for cementing substances in the form of silica precipitations was tried by analyzing arbitrarily selected 3x5 µm^2 large areas of ultrathin sections cut from a sample heated to 200°C (Test LD14). The selected area is depicted in Fig 26, while closing up gave the detailed view in Fig 27, which shows the location of five spots for point analyses. A typical spectrum showing the major peaks for Si and Al is given in Fig 28, the Al/Si-ratio typically being in the range of 0.34-0.40 for montmorillonite as concluded from comprehensive element analyses.

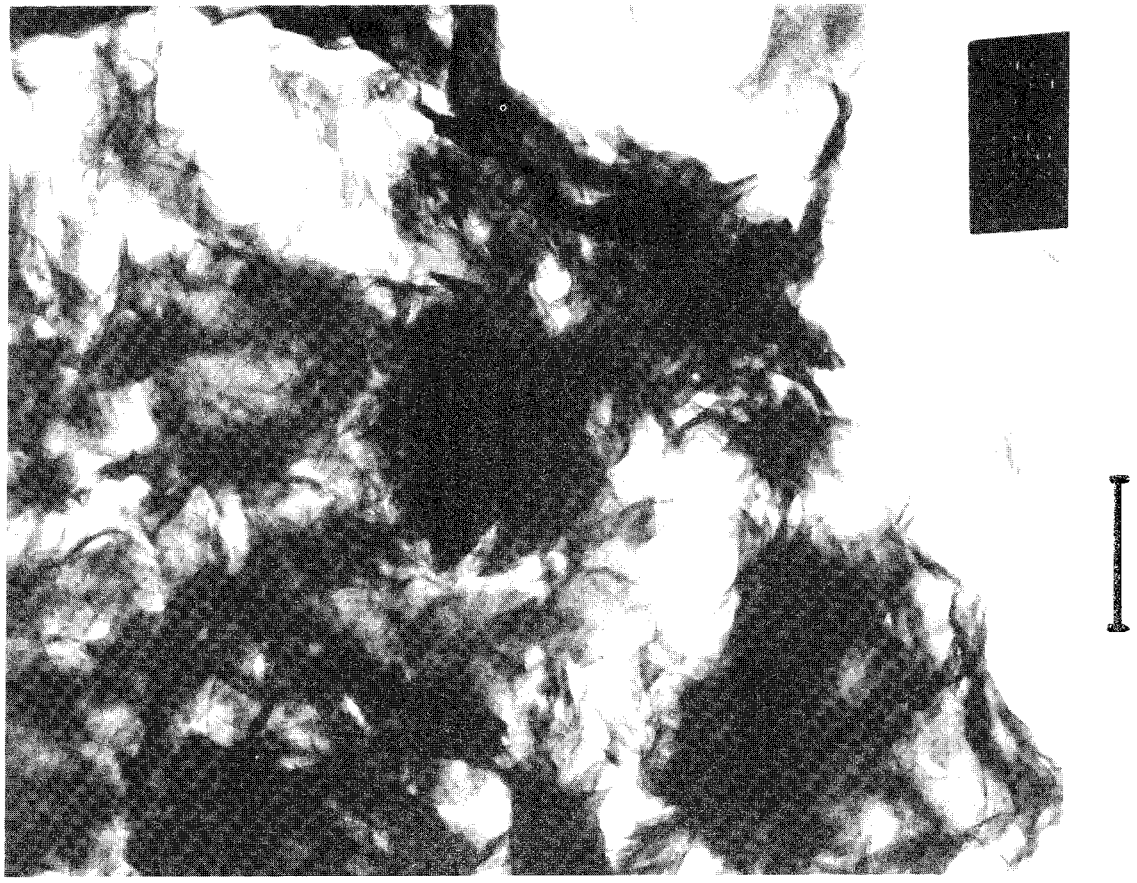

Fig 23. TEM picture of vapor-treated SWY-1 clay showing strong aggregation and collapse of montmorillonite stacks. The scale is 4 μm

Silica precipitations are naturally expected to show significantly lower values and we see from Table 5 that one of the spots, i.e. the one termed "1", may represent such a silica particle. Naturally, this could not be safely decided without extending the number of analyses and relating the chemical composition to the electron-optical image. Element mapping was therefore applied to get detailed information on the areal distribution of silica and aluminum. Magnesium, iron, and potassium, which we also assumed to be of interest in the present context, were also mapped.

Fig 29 shows the results of the mappings of silica and aluminum superimposed on the image, each individual point covering 70 Å x 70 Å and spectra being collected in 100 milliseconds. The total investigated area was therefore only about 15 μm^2, from which one concludes that mapping of large areas is very time-consuming.

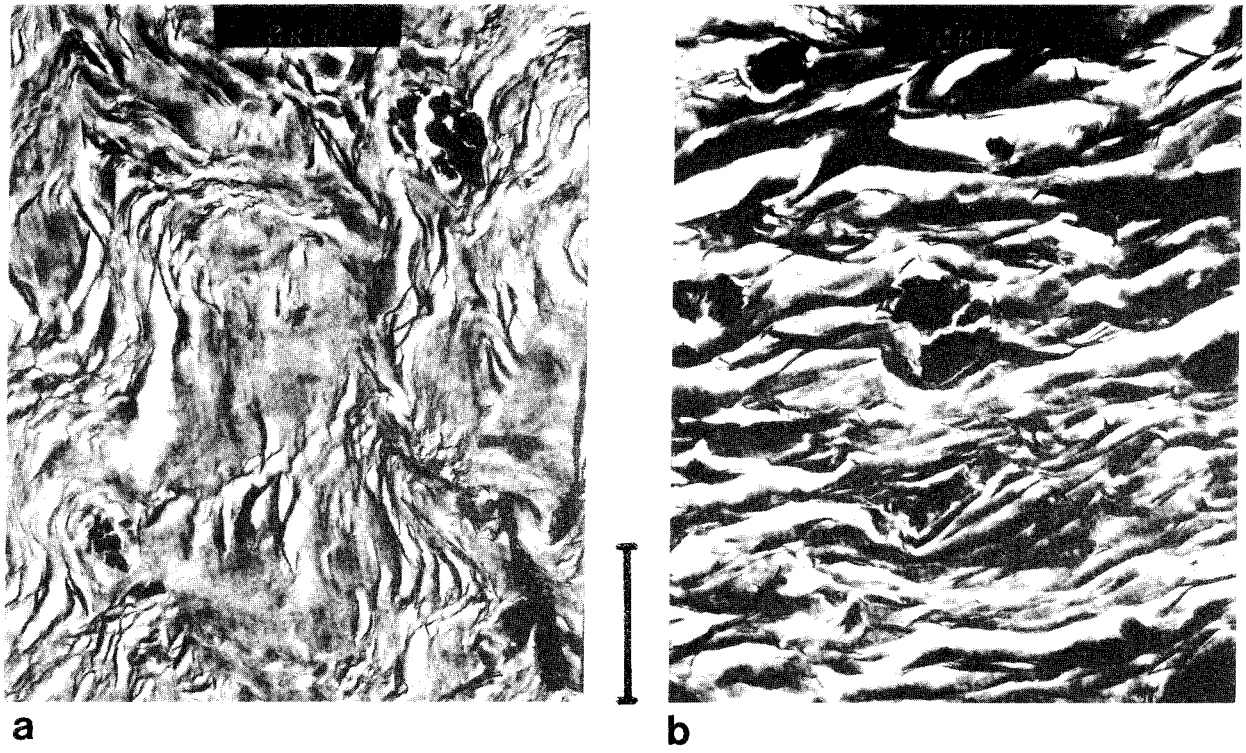

Fig 24. TEM micrograph of dense SWY-1 clay ($\rho_d = 1.59$ g/cm^3). a) unheated reference sample, b) sample heated to 150°C for 1 year

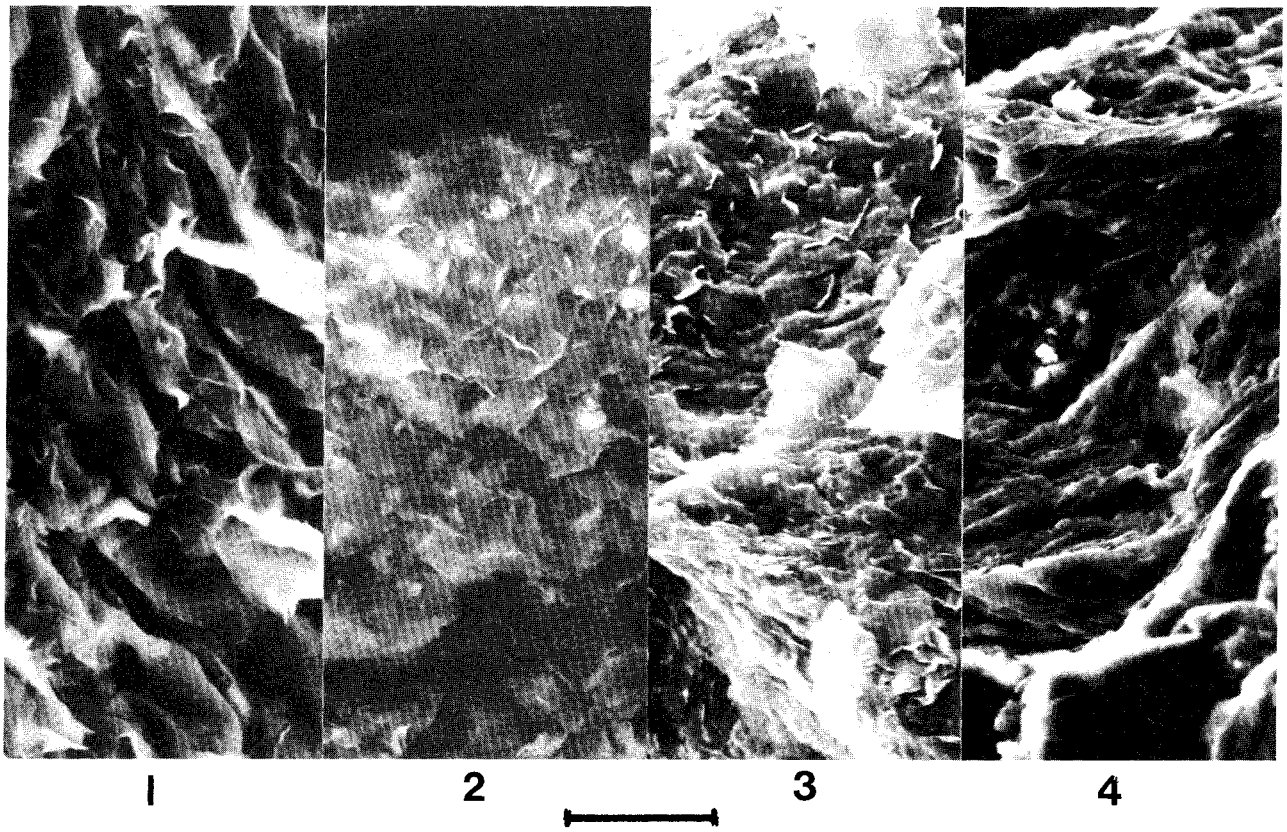

Fig 25. SEM micrograph panorama showing the surface character of SWY-1 clay. 1) Unheated, 2) 105°C, 3) 150°C, 4) 200°C

Table 5. Point element analyses of areas 1-5. Concentrations relative to silica

Area	Element	Peak/window ratio for Si = 1.0000
1	Mg	0.00
2		0.06
3		0.06
4		0.06
5		0.04
1	Al	0.05
2		0.40
3		0.35
4		0.37
5		0.36
1	Fe	0.01
2		0.05
3		0.07
4		0.07
5		0.06
1	K	0.01
2		0.01
3		0.04
4		0.01
5		0.01

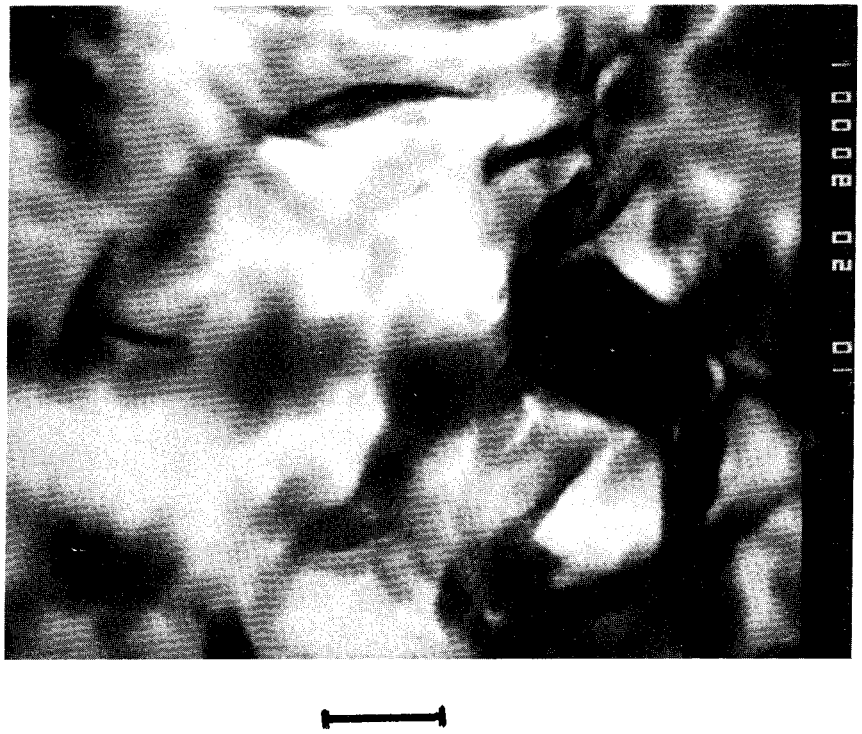

Fig 26. TEM pictures showing porous part of ultrathin section of dense SWY-1 clay heated to 200°C for 0.5 years. The scale is 1 µm

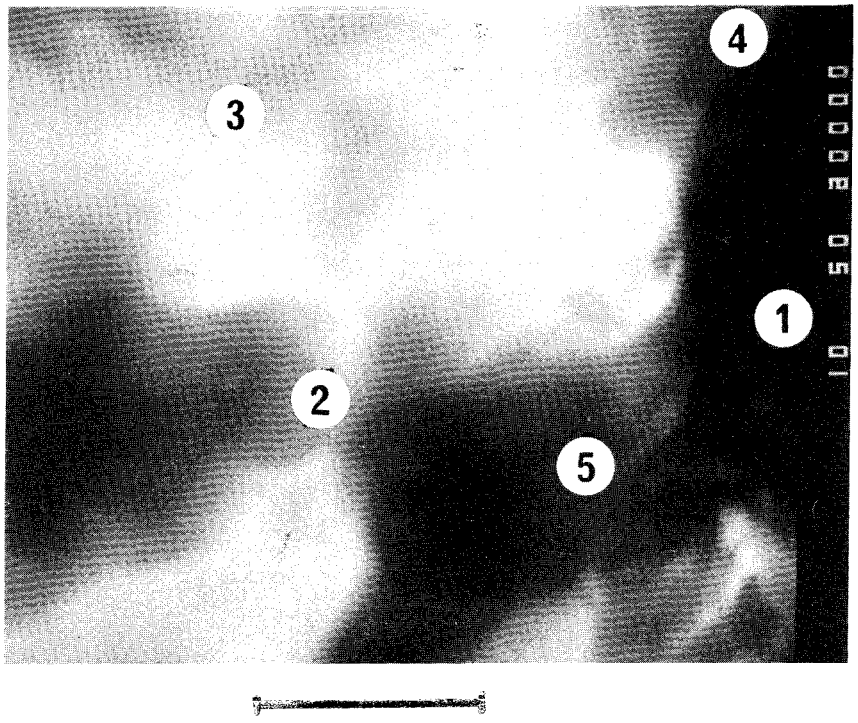

Fig 27. Detail of micrograph in Fig 25 with location of selected areas for element analysis. The scale is 1 µm

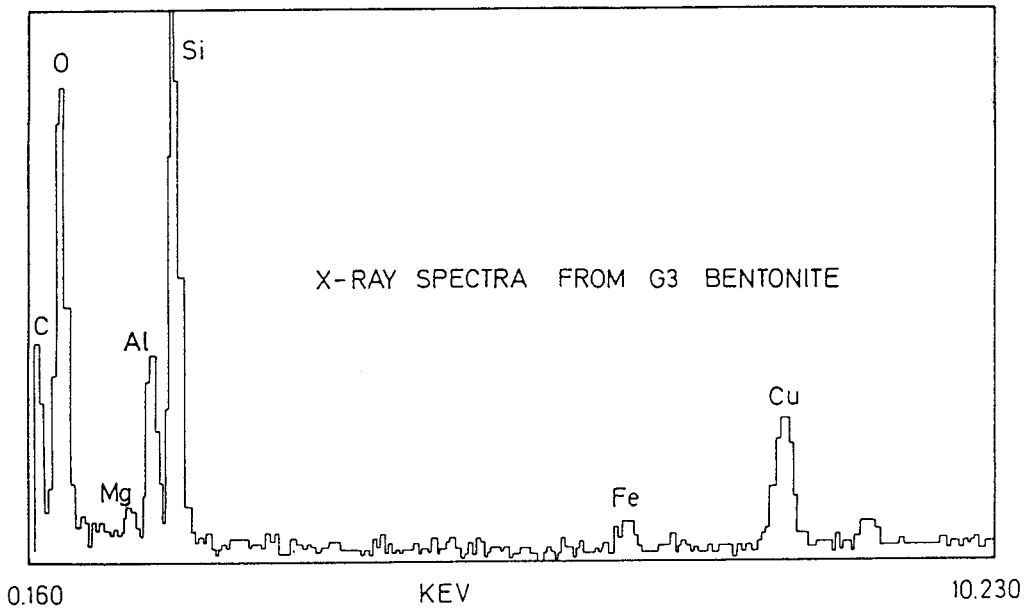

Fig 28. EDX spectrum of typical montmorillonite

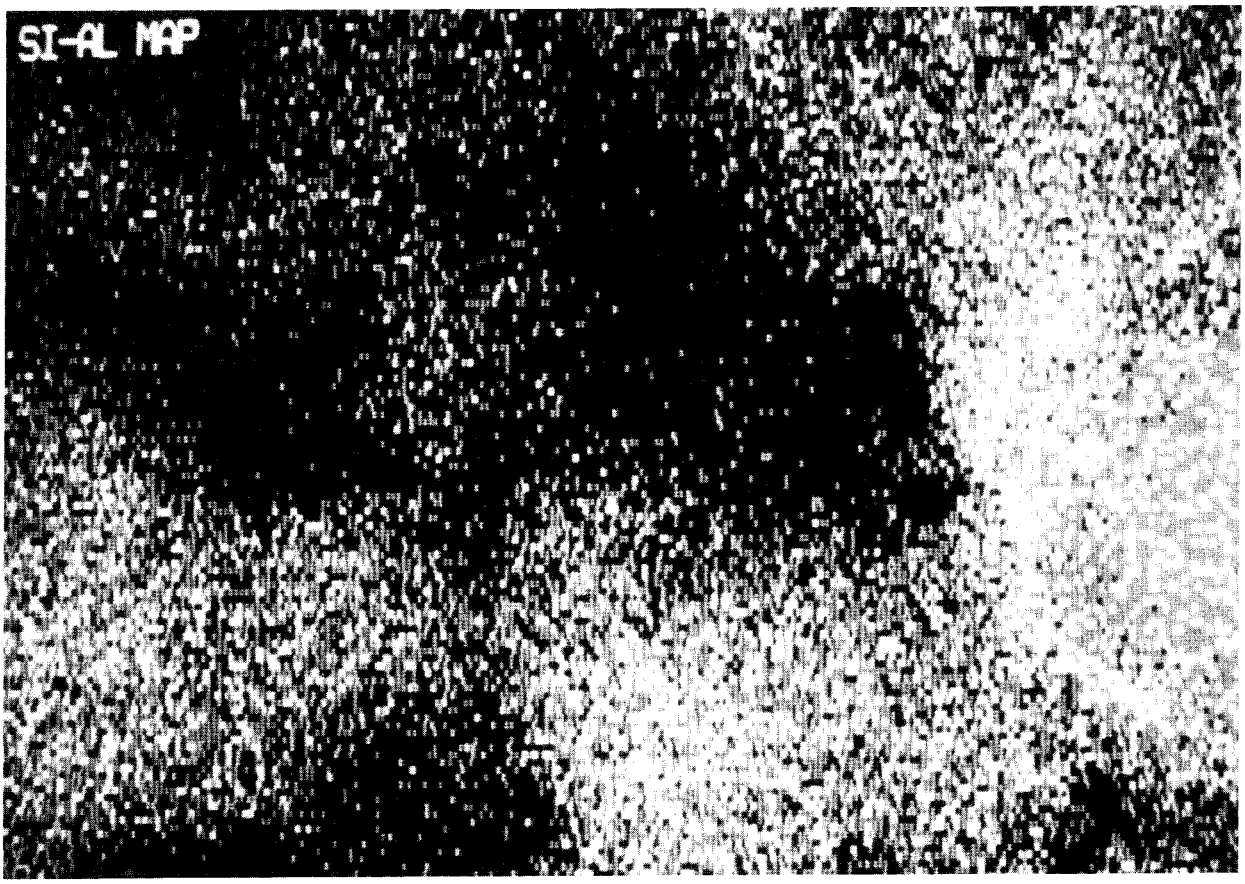

Fig 29. Mapping of Si and Al superimposed on the image (cf. Fig 27). White areas represent typical Si/Al ratio of montmorillonite, while grey areas show excess Si. The silica grain at the right border is obvious, silica-enriched zones are seen at the edges of several aggregates

We see from the figures that silica and aluminum were equally distributed over large areas with the exception of the dense body ("1") at the right border of the micrograph of Fig 27, and possibly also at the upper edges of the aggregates termed 2 and 5 in the same picture. In the dense body, and to some extent in the last-mentioned parts, silica was clearly in excess. It is a well established fact that ultramicrotome cutting of quartz particles is not possible, which indicated that the silica-rich bodies must have had a low shear resistance and that they consisted of hydrated, amorphous silica gel material. Electron diffraction confirmed that the silica-rich substances were not or only weakly crystalline, but variation of the electron beam intensity revealed that the larger body contained a couple of small, dense quartz or cristobalite particles, which may possibly have served as condensation nuclei at the precipitation of the amorphous silica. SEM executed on fractured, freeze-dried and uncoated clay clearly showed features that could be compatible with precipitations as nodules and brims at the surface of clay aggregates of the sort found in the element mapping of ultrathin sections but element analysis have not yet been made for confirmation.

It is concluded from this pilot test that Si was really released on heating of soft montmorillonite clay and that the identified amorphous silica compounds were closely integrated in the system of large neighboring clay aggregates. As stated previously, the silica may have been dissolved in the electrolyte-free porewater in the heating period and precipitated on cooling. If open sample holders had been used in conventional autoclaves it would not have been detected.

A corresponding study of dense SWY-1 clay was conducted in Sweden in spring 1988 with the intention to identify whether release and precipitation of silica is associated with a certain critical temperature and if the release is a time-dependent, Arrhenius-type effect. The study, which concerned samples from Tests HD2 (reference), H9 9-10 and HD 12-17 (cf Table 3), included point element analyses as well as mapping and electron diffractometry of opaque inclusions in the same way as described in the preceding text. The major observations can be summarized in the following way:

1. HD2, Reference sample (20°C)

   Amorphous matter was not found to be present but widely scattered quartz particles smaller than 1 µm could be seen. Groups of very small,

opaque bodies were noticed in larger pores but they were vaporized on exposure to the radiation

2. HD 14-17, Hydrothermal treatment during 1 week to 1 month (105-130°C)

A few amorphous precipitations with excess silica and sized 1-2 µm were found in larger voids

3. HD 12 & 13, Hydrothermal treatment during 1 week to 1 month (160°C)

Opaque, amorphous bodies with an obvious amount of excess silica and with about 1 µm diameter, were rather frequent

4. HD 9 & 10, Hydrothermal treatment during 1 week to 1 month (200°C)

Large silica-rich, amorphous bodies ($\leq$2.5 µm) with the same frequency as in the 160°C samples were identified (Fig 30). Variation in focusing revealed that the precipitation had taken place on one or several small quartz nuclei. The largest bodies appeared to occupy the major part of certain wide voids. The microstructure of the clay matrix surrounding such voids was found to be characterized by a significantly larger space between aligned branches of flakes than further off from the voids. The most probable explanation of this effect is that the precipitated silicious substance in the voids extends to a shallow depth into the surroundings from where it stems, cementing the flakes together or preventing them from expanding by blocking the periphery of the stacks.

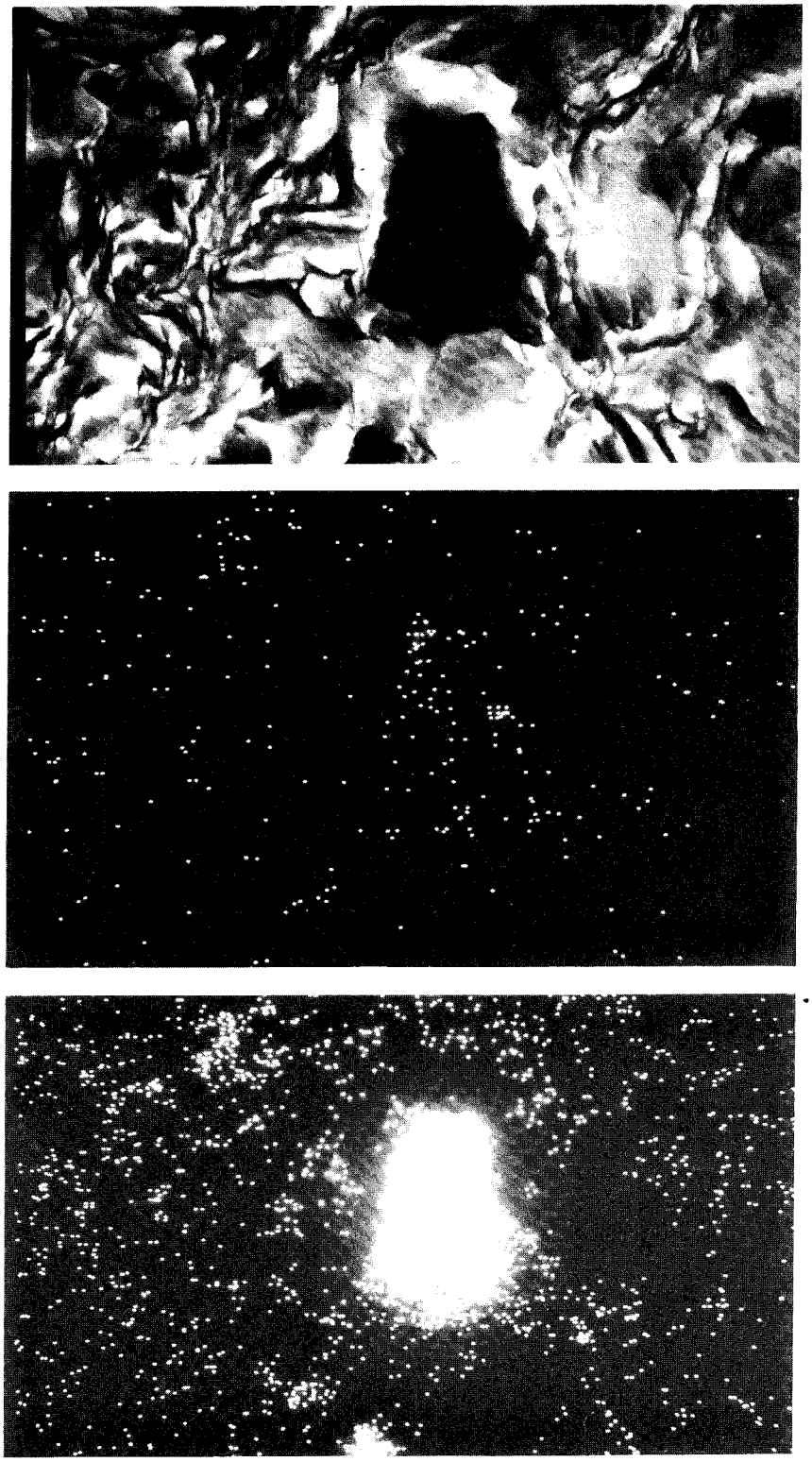

Fig 30. STEM pictures showing typical large amorphous precipitate in sample HD 10. Upper: TEM image. Center: Al mapping showing typical concentration level for montmorillonite. Lower: Mapping showing strong excess of Si. The scale is 1 μm

6 DISCUSSION

6.1 GENERAL

The applied technique for conducting hydrothermal tests of Na montmorillonite samples was found to be be useful although larger sample cells in which the pore-water pressure can be controlled with better accuracy would be preferable. A new generation of cells has actually been designed and tested and found to be very useful.

As to the applied analyses it is concluded that XRD testing in its common forms is of limited value for identification of mineral alteration. High resolution STEM appears to be the best analyzing tool for very detailed studies of various alteration processes. It is highly recommended for future use.

Ordinary high resolution TEM for microstructural quantification is very valuable and both preparation techniques and methods and parameters for evaluation and characterization are now available.

SEM with its low resolution power and unability to yield micrographs that can be used for quantitative microstructural analysis, should only be used for special purposes, like identification of the physical shape of large precipitations and determination of their chemical nature through element analysis.

The rheological testing appears to be one of the most sensitive bulk test methods and, applying recently obtained results from parallel research projects, it is suggested that creep tests be introduced as well. This can easily be made by using samples extruded from the large cells mentioned above.

6.2 SILICA RELEASE AND PRECIPITATION

Direct, comprehensive information on this issue is obtained from the STEM investigation, while ordinary TEM and rheology studies yielded indirect supporting data. The microscopy gave definite information that silica was actually released on heating to 150-200°C and that reformation of silica compounds, probably in the form of precipitated hydrous silica gels ($H_4SiO_4 \cdot H_2O$), took place on cooling.

The precipitations appeared as local, relatively large bodies in the open voids of the water saturated clay of low density, which suggests that they should have little effect on the strength properties of such clays. This is supported by the fact that the ultimate strength of the 200°C sample was almost the same as that of the 105 and 150°C samples. Since the precipitations were found to be intimately integrated with the clay matrix in the dense clay, they were very probably the major source of the drastic strengthening of this clay on heating to 150-200°C. It is reasonable to believe that the significant stiffening on heating beyond 150°C was mainly due to cementation caused by silica precipitation, while the less dramatic but still appreciable stiffening that appeared on heating to 105-130°C mainly resulted from microstructural alteration.

It is obvious that the effect of cementation through precipitation of released silica in repository environment is controlled by the concentration of dissolved silica in the groundwater. Thus, the matter of silica migration and possible precipitation in water saturated montmorillonite clay can only be treated by considering the geochemical conditions in the host rock. If silica is free to migrate out of the clay, which would be effectively assisted by the temperature gradient, we expect that only microstructural changes affect the rheology and the swelling and gel-forming ability of the clay.

6.3 MINERAL ALTERATION

Taking the XRD tests as a basis one would conclude that 10 Å minerals were formed in small quantities, i.e. up to 10 %, in the clays heated to 200°C. Very probably, the appearance of 10 Å basal spacing in the dense Na montmorillonite was due to permanent collapse of dehydrated montmorillonite or beidellite, while it may be indicative of illite in the soft KCl-soaked clay. We conclude that the actual content of 10 Å minerals is on this order in the soft clay and that they may well be illite. However, the dense KCl-soaked clay was estimated to have a lower content of such minerals, which may be explained by a hindered uptake of potassium ions due to effective silica gel blocking at the periphery of the stacks. Such blocking would naturally be much more frequent in the dense clay, where the silica precipitates were integrated in the clay matrix, than in the soft clay where these compounds accumulated in larger voids.

In this context it should be mentioned that Pytte's theory on smectite/illite conversion yields results that are on the right order of magnitude for the soft clay. Thus, assuming that the charge change leading to beidellite follows the same rate process at the illite conversion and that the potassium was very rapidly absorbed under the prevailing post-heating conditions, Pytte's diagram suggests that at least 15 % illite would be formed in 0.5 years at 200°C. The lack of agreement for the dense clay suggests that the conversion process cannot be correctly described by use of this theory.

Careful interpretation of XRD plots of Na montmorillonite heated to 150°C for 0.5 and 1 year, respectively, showed no sign of 10 Å minerals. This may indicate that permanent collapse of the montmorillonite stacks associated with dehydration and silica release is not an Arrheniusian process but related to heating to a certain critical temperature which may be about 200°C.

Taking into account also the fact that silica was released in quantities that may have been as much as 25 % of the initial lattice silica, we conclude that beidellitization probably occurred at temperatures exceeding 150°C. A working hypothesis is that this process is associated with heat-induced conversion of the montmorillonite from a low-temperature form, of which the EF model may be representative, to a high-temperature state of the HEW-type. No safe conclusions can be drawn until relevant crystal lattice investigations have been made, using MAS/NMR and other suitable techniques.

6.4 MICROSTRUCTURAL CHANGES

Heat-induced microstructural changes in the form of collapse of interlamellar hydrates and "syneresis"-type contraction of the particle network to form stronger, continuous branches with larger voids in between, were documented for all the heating stages. Due to rehydration in the cooling state, the heat-induced contraction of the stacks and the associated reshaping of these structural components, the actual microstructural alteration on heating is probably somewhat more comprehensive in the heated state than recorded by the micrographs. This should be further investigated by correlating microstructural data with conductivity and diffusion data.

It is logical to believe that the stiffening observed in the rheology tests for temperatures lower than 150°C was largely due to the microstructural reorganization. The fact that the porewater pressure was low in most of these tests demonstrates that this pressure does not need to be high to produce dehydration or any other microstructural change.

The conclusion from the simple rheological tests and the microscopy that release of significant quantities of silica takes place quickly, has been reconfirmed by creep tests of large samples obtained by using a new type of cell with a diameter and length of 20 mm. MX-80 Wyoming Na bentonite with a dry density of 1.35 g/cm^3 was saturated with distilled water and heated to 250°C for 3 weeks at a porewater pressure of about 3 MPa. The diagram in Fig 31 shows the very obvious drop in shear strain and strain rate on heating, the major part of the strengthening being ascribed to cementation by precipitated silica compounds. The shear stress was 260 kPa, which is about 80 % of the shear strength of the unheated reference clay.

6.5 PRELIMINARY CONCLUSIONS

6.5.1 Outline of model of hydrothermal effects on water saturated Na montmorillonite clay

The effects of heating, i.e. the temperature-related contraction of previously expanded montmorillonite stacks and dispersed particle network branches, and the release of silica associated with transfer from montmorillonite to beidellite, are schematically illustrated in the form of tentative scenarios in Figs 32 and 33 for potassium-poor porewater. The various contraction stages are related to temperatures that are not yet safely established, while the last dehydration phase leading to collapse to 10 Å and release of silica, is documented to take place in the temperature range of 150-200°C. This latter stage is assumed to yield transfer from montmorillonite to beidellite. It is assumed that rehydration yielding the initial 2-3 hydrates in interlamellar positions takes place on cooling except for some permanent closure in material heated to 150-200°C. The original microstructure is, however, never recovered.

The detailed mechanisms involved in uptake of potassium and conversion to illite have not yet been revealed. It is estimated that they are very much related to the

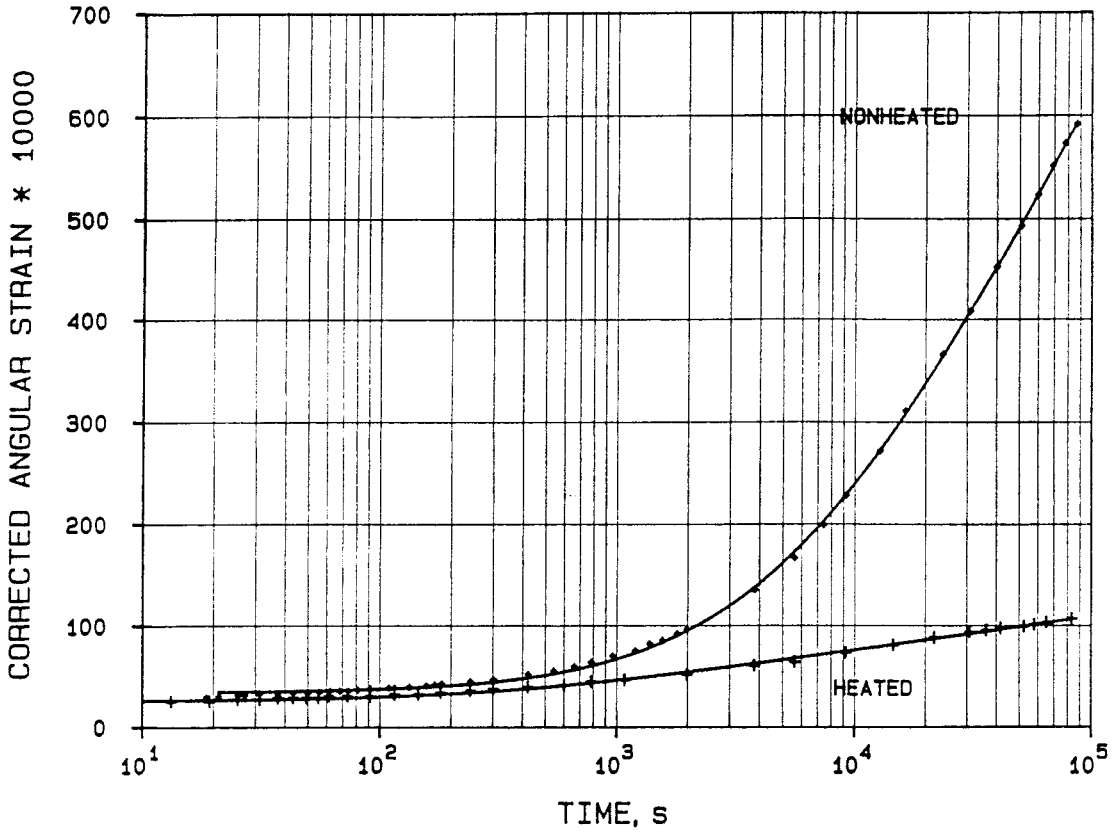

Fig 31. Creep curves for MX-80 bentonite with a dry density of 1.35 g/cm3. Upper curve relates to unheated material, while the lower curve represents clay heated at 250°C for 3 weeks at a porewater pressure of about 3 MPa

heat-induced contraction and silica precipitation and continued research is expected to deepen the understanding also in this respect, especially if hydro-thermal tests with porewaters of various composition are included.

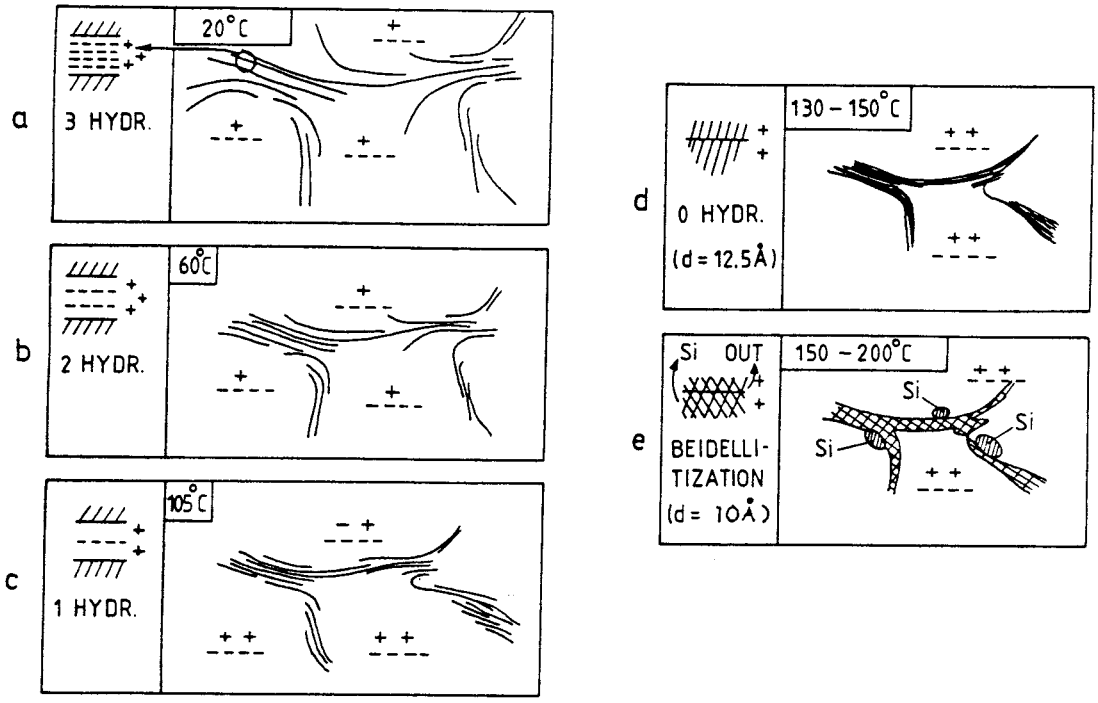

Fig 32. Schematic tentative model of microstructural changes and silica release at low bulk density

6.5.2 Special effects on non-saturated Na montmorillonite clay

At a relatively low degree of water saturation the silica release at about 200°C is expected to yield precipitation of cementing compounds at any porewater composition, simply because the solubility of silica will be exceeded. Since larger voids contain vapor, the precipitates are formed in the clay complexes, yielding more effective cementation than in water saturated clay. This may offer an explanation of the "Couture effect", i.e. the empirical finding that vapor-treated montmorillonite rapidly looses a significant part of its expandability already at about 150°C (34).

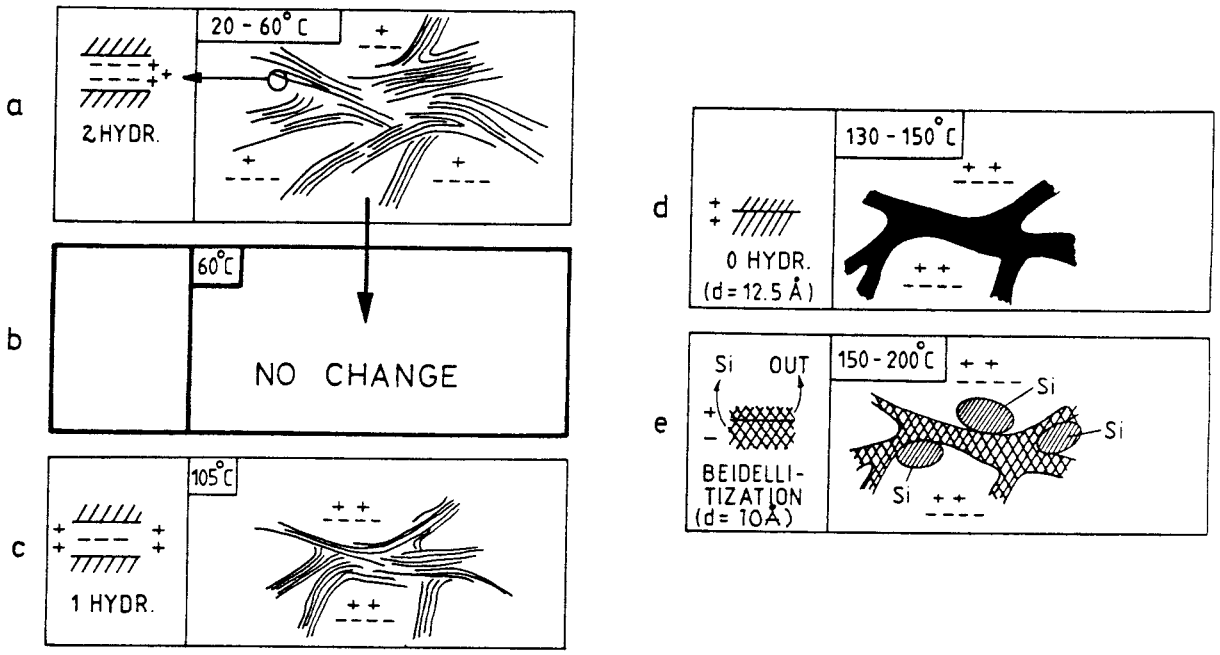

Fig 33. Schematic tentative model of microstructural changes and silica release at high bulk density

7 ACKNOWLEDGEMENTS

The authors like to express their gratitude to Professor Necip Güven for the pilot STEM study at Texas Tech, Lubbock, and to Dr Rolf Odselius, Dep of Pathology, University of Lund, for valuable assistance in running the SEM study. Thanks are extended to Professor Anders Andersson and his group, Dep of Histology, University of Lund for the ultramicrotomy and assistance in the TEM study, and to Dr Reine Lindwall, Linköping University, for the larger part of the STEM analyses.

Moreover, the authors wish to express their appreciation to Mikael Erlström and Jeanette Stenelo, Swedish Geological and Ideon Research Center, respectively, for support in the preparation of the report.

8 REFERENCES

1 Anderson, D.M. Smectite Alteration. SKBF/KBS Technical Report 83-03, 1983

2 Hower, J., Exinger, E., Hower, M., and Perry, E. The Mechanism of Burial Diagenetic Reactions in Argillaceous Sediments. I. Mineralogical and Chemical Evidence. Geol. Soc. Amer. Bull. Vol. 87, 1976 (pp. 725-737)

3 Boles, J.R. and Franks, S.G. Clay Diagenesis in Wilcox Sandstones of Southwest Texas: Implications of Smectite Diagenesis on Sandstone Cementation. J. Sed. Petrol. Vol. 49, 1979 (pp. 55-70)

4 Sposito, G. The Polymer Model of Thermochemical Clay Mineral Stability. Clays and Clay Minerals, Vol. 34, No. 2, 1986 (pp. 198-203)

5 Tardy, Y. & Touret, O. Hydration Energies of Smectites. A Model for the Glauconite, Illite, and Corrensite Formation. Instit. de Géologie, Univ. Louis Pasteur and Centre de Sédimentologie, Strasbourg. Int Rep. 1986

6 Pollastro, R.M. Mineralogical and Morphological Evidence for the Formation of Illite at the Expense of Illite/Smectite. Clays and Clay Minerals, Vol. 33, 1985 (pp. 265-274)

7 Nadeau, P.H., Wilson, M.J., McHardy, W.J., and Tait, J.M. The Conversion of Smectite to Illite During Diagenesis: Evidence From some Illitic Clays from Bentonites and Sandstones. Mineral. Mag. Vol. 49, 1985 (pp. 393-400)

8 Inoue, A., Kohyama, N., Kitagawa, R. & Watanabe, T. Chemical and Morphological Evidence for the Conversion of Smectite to Illite. Clays and Clay Minerals, Vol. 35, No. 2, 1987 (pp. 111-120)

9 Güven, N., Carney, L.L., and Ridpath, B.E. Evaluation of Geothermal Drilling Fluids Using a Commercial Bentonite and a Bentonite/-Saponite Mixture. Contr. Rep. Sand 86-7180, SANDIA Nat. Laboratories, Albuquerque, New Mexico, USA, 1987

10 Pytte, A.M. The Kinetics of the Smectite to Illite Reaction in Contact Metamorphic Shales. M.A. Thesis, Dartmonth College, Hanover, N.H., 1982

11 Bannister, R.A. Brammalite (Sodium Illite) a New Mineral from Llandebie, South Wales. Mineralogical Magazine, Vol. 26, 1943 (pp. 304-307)

12 Frey, A. A Mixed-layer Paragonite-Phengite of Low-grade Metamorphic Origin. Contribution of Mineral Petrology, Vol. 24, 1969 (pp. 63-65)

13 Lasaga, A.C. Rate Laws of Chemical Reactions. Kinetics of Geochemical Processes. (Ed:s Lasaga and Kirkpatrick). Mineral. Soc. of America, Vol. 8, 1981 (pp. 1-67)

14 Eberl, D.D. & Hower, J. Kinetics of Illite Formation. Bull. Geol. Soc. Amer. Vol. 87, 1976 (pp. 1326-1330)

15 Robertson, H.E., & Lahann, R.W. Smectite to Illite Conversion Rates: Effects of Solution Chemistry. Clays and Clay Minerals, Vol. 29, 1981 (pp. 129-135)

16 Howard, J.J. and Roy, D.M. Development of Layer Charge and Kinetics of Experimental Smectite Alteration. Clays and Clay Minerals, Vol. 33, No. 2, 1985 (pp. 81-88)

17 Pusch, R., Hökmark, H. & Börgesson, L. Outline of Models of Water and Gas Flow Through Smectite Clay Buffers. SKB Technical Report 87-10, 1987

18 Pusch, R. Stability of Deep-Sited Smectite Minerals in Crystalline Rock - Chemical Aspects. SKBF/KBS Technical Report 83-16, 1983

19 Byström, A:M. Mineralogy of the Ordovician Bentonite Beds at Kinnekulle, Sweden. Sveriges Geol. Unders. Ser. C. No. 540, 1956

20 Velde, B. & Brusewitz, A.M. Metasomatic and Non-metasomatic Low Grade Metamorphism of Ordovician Meta-bentonites in Sweden. Geochimica et Cosmochimica Acta, Vol. 46, 1982 (pp. 447-452)

21 Pusch, R. Final Report on the Buffer Mass Test - Volume III: Chemical and Physical Stability of the Buffer Materials. Stripa Project Technical Report 85-14, 1985

22 Pusch, R. Identification of Na-smectite Hydration by use of "Humid Cell" High Voltage Microscopy. Appl. Clay Science, Vol. 2, 1987 (pp. 343-352)

23 Forslind, E. & Jacobsson, A. Water, a Comprehensive Treatise. Plenum Press, 1975

24 Sposito, G. & Prost, R. Structure of Water Adsorbed on Smectites. Chemical Reviews, Vol. 82, No. 6, 1982 (pp. 553-573)

25 Pusch, R. Permanent Crystal Lattice Contraction - A Primary Mechanism in Thermally Induced Alteration of Na Bentonite. Materials Research Society Proc. Vol. 84, Scientific Basis for Nuclear Waste Management X, J.K. Bates and W.B. Seefeldt, editors, 1987 (pp. 791-802)

26 Anderson, D.M. & Tice, A.R. Low-temperature Phases of Interfacial Water in Clay-Water Systems. Soil Science of America. Proc. Vol. 35, No. 1, 1971

27 Colton-Bradley, V.A. The Role of Pressure in Smectite Dehydration - Effects on the Smectite-to-Illite Transformation and Geopressure Development. Branch of Oil and Gas Resources, U.S. Geological Survey, Denver, USA, 1986

28 Frenkel, J. Kinetic Theory of Liquids. Clarendon Press, Oxford, 1946

29 Houwink, R. Elastizität/Plastizität und Struktur der Materie. Verl. Th. Steinkopff, Dresden & Leipzig, 1958

30 Carlsson, T. Interactions in MX-80 Bentonite/Water/Electrolyte Sys-

tems. Dort. Thesis, Luleå Univ. of Techn., Luleå 1986:55D (pp. 68-70)

31 Pusch, R. Swelling Pressure of Highly Compacted Bentonite. SKBF/KBS Technical Report 80-13, 1980

32 Jones, R.C. & Nehara, G. Amorphous coatings on Mineral Surfaces. Soil Sci. Soc. America, Proc., Vol. 37, 1973 (pp. 792-798)

33 Bennet, R.H. & Hulbert, M.H. Clay Microstructure. Int. Human Resources Dev. Corp., Boston/Houston/London, 1986

34 Couture, R.A. Steam Rapidly Reduces the Swelling Capacity of Bentonite Nature, Vol. 318, 1985 (pp. 50-52)

List of SKB reports

Annual Reports

1977–78
TR 121
KBS Technical Reports 1 – 120.
Summaries. Stockholm, May 1979.

1979
TR 79–28
The KBS Annual Report 1979.
KBS Technical Reports 79-01 – 79-27.
Summaries. Stockholm, March 1980.

1980
TR 80–26
The KBS Annual Report 1980.
KBS Technical Reports 80-01 – 80-25.
Summaries. Stockholm, March 1981.

1981
TR 81–17
The KBS Annual Report 1981.
KBS Technical Reports 81-01 – 81-16.
Summaries. Stockholm, April 1982.

1982
TR 82–28
The KBS Annual Report 1982.
KBS Technical Reports 82-01 – 82-27.
Summaries. Stockholm, July 1983.

1983
TR 83–77
The KBS Annual Report 1983.
KBS Technical Reports 83-01 – 83-76
Summaries. Stockholm, June 1984.

1984
TR 85–01
Annual Research and Development Report 1984
Including Summaries of Technical Reports Issued during 1984. (Technical Reports 84-01– 84-19)
Stockholm June 1985.

1985
TR 85-20
Annual Research and Development Report 1985
Including Summaries of Technical Reports Issued during 1985. (Technical Reports 85-01-85-19)
Stockholm May 1986.

1986
TR 86-31
SKB Annual Report 1986
Including Summaries of Technical Reports Issued during 1986
Stockholm, May 1987

1987
TR 87-33
SKB Annual Report 1987
Including Summaries of Technical Reports Issued during 1987
Stockholm, May 1988

Technical Reports

1988
TR 88-01
Preliminary investigations of deep ground water microbiology in Swedish granitic rocks
Karsten Pedersen
University of Göteborg
December 1987

TR 88-02
Migration of the fission products strontium, technetium, iodine, cesium and the actinides neptunium, plutonium, americium in granitic rock
Thomas Ittner[1], Börje Torstenfelt[1], Bert Allard[2]
[1]Chalmers University of Technology
[2]University of Linköping
January 1988

TR 88-03
Flow and solute transport in a single fracture. A two-dimensional statistical model
Luis Moreno[1], Yvonne Tsang[2], Chin Fu Tsang[2], Ivars Neretnieks[1]
[1]Royal Institute of Technology, Stockholm, Sweden
[2]Lawrence Berkeley Laboratory, Berkeley, CA, USA
January 1988

TR 88-04
Ion binding by humic and fulvic acids: A computational procedure based on functional site heterogeneity and the physical chemistry of polyelectrolyte solutions
J A Marinsky, M M Reddy, J Ephraim, A Mathuthu
US Geological Survey, Lakewood, CA, USA
Linköping University, Linköping
State University of New York at Buffalo, Buffalo, NY, USA
April 1987

TR 88-05
Description of geophysical data on the SKB database GEOTAB
Stefan Sehlstedt
Swedish Geological Co, Luleå
February 1988

TR 88-06
Description of geological data in SKBs database GEOTAB
Tomas Stark
Swedish Geological Co, Luleå
April 1988

TR 88-07
Tectonic studies in the Lansjärv region
Herbert Henkel
Swedish Geological Survey, Uppsala
October 1987

TR 88-08
Diffusion in the matrix of granitic rock. Field test in the Stripa mine. Final report.
Lars Birgersson, Ivars Neretnieks
Royal Institute of Technology, Stockholm
April 1988

TR 88-09
The kinetics of pitting corrosion of carbon steel. Progress report to June 1987
G P Marsh, K J Taylor, Z Sooi
Materials Development Division
Harwell Laboratory
February 1988

TR 88-10
GWHRT – A flow model for coupled groundwater and heat flow
Version 1.0
Roger Thunvik[1], Carol Braester[2]
[1] Royal Institute of Technology, Stockholm
[2] Israel Institute of Technology, Haifa
April 1988

TR 88-11
Groundwater numerical modelling of the Fjällveden study site – Evaluation of parameter variations
A hydrocoin study – Level 3, case 5A
Nils-Åke Larsson[1], Anders Markström[2]
[1] Swedish Geological Company, Uppsala
[2] Kemakta Consultants Co, Stockholm
October 1987

TR 88-12
Near-distance seismological monitoring of the Lansjärv neotectonic fault region
Rutger Wahlström, Sven-Olof Linder, Conny Holmqvist
Seismological Depertment, Uppsala University, Uppsala
May 1988

TR 88-13
Validation of the rock mechanics HNFEMP code against Colorado school of mines block test data
Ove Stephansson, Tomas Savilahti
University of Luleå, Luleå
May 1988

TR 88-14
Validation of MUDEC against Colorado school of mines block test data
Nick Barton, Panayiotis Chryssanthakis, Karstein Monsen
Norges Geotekniske Institutt, Oslo, Norge
April 1988